Available online at www.sciencedirect.com
SCIENCE DIRECT®
Journal of Computational Physics 195 (2004) 528–559
JOURNAL OF COMPUTATIONAL PHYSICS
www.elsevier.com/locate/jcp

A thermodynamically consistent and fully conservative treatment of contact discontinuities for compressible multicomponent flows

Shao-Ping Wang *, Mark H. Anderson, Jason G. Oakley, Michael L. Corradini, Riccardo Bonazza *

Department of Engineering Physics, Fusion Technology Institute, University of Wisconsin-Madison, Madison, WI 53706, USA

Received 10 October 2002; received in revised form 23 October 2003; accepted 23 October 2003

Abstract

A thermodynamically consistent and fully conservative (TCFC) treatment of contact discontinuities (designated as TCFC model in this paper) is proposed for the simulation of compressible multicomponent flows with shock-interface interactions, yielding an accurate capture of contact discontinuities. Starting from the total energy equation of the mixture, a new formulation is developed to define the ratio of specific heats of the mixture, and a governing equation in conservative form for the pressure is subsequently obtained. Another formulation is derived to determine the molecular weight of the mixture from classical thermodynamics. The governing equations in conservative form are further derived to calculate the specific heats ratio and the molecular weight of the mixture with their new formulations and the continuity or mass fraction equations for the individual components. Finally, the governing equations for the ratio of specific heats, the molecular weight and the pressure, combined with the continuity and momentum equations, offer the new hyperbolic conservation laws for the description of multicomponent or multifluid flows with shock-interface interactions. A simple version of the model is also developed without solving the governing equation for the molecular weight of the mixture. A brief analysis of the numerical uncertainties of conventional conservation models and the present TCFC models is presented and the consistency of any additional equation derived within any model with the initial governing equations is investigated. An analysis of the proposed TCFC model and the conventional conservative models is also performed on the pressure evolution for a mixture associated with isolated contact discontinuities. The results show that the present TCFC model produces a uniform pressure field and thus the pressure maintains in equilibrium across the material interfaces. The proposed TCFC model is then implemented into a Godunov-type method based upon a fast, exact Riemann solver. Several multicomponent flow problems with both strong and weak shocks are simulated using this new model and conventional conservation models, and comparisons of the numerical results from the various models and, where possible, exact solutions are performed. It is shown that the proposed TCFC model can handle both strong and weak shocks, and that the numerical solutions are completely oscillation-free through the contact discontinuities. This new approach offers a suitable treatment of contact discontinuities for compressible multicomponent flows and also maintains all the favorable features of fully conservative conservation

* Corresponding authors. Tel.: +608-265-9469; fax: +608-263-7451.
E-mail addresses: wang@engr.wisc.edu (S.-P. Wang), manderson@engr.wisc.edu (M.H. Anderson), oakley@engr.wisc.edu (J.G. Oakley), corradini@engr.wisc.edu (M.L. Corradini), bonazza@engr.wisc.edu (R. Bonazza).

doi:10.1016/j.jcp.2003.10.010

laws. It belongs to the conservative approaches and is independent of numerical schemes. From the analysis of the numerical uncertainties of several models proposed in the past and the present numerical experiments, it is determined that the conservative or non-conservative form of some additional governing equations is not the ultimate reason that produces oscillating solutions near the material interfaces. The main cause of the oscillating solutions with conventional conservation models is the inappropriate determination of the ratio of specific heats of the mixture. Oscillation-free results are obtained for two test cases with weak shocks even with conventional conservation models using the present Godunov-type method based on a fast exact Riemann solver. This suggests that the problems with weak shocks and strong post-shock contact discontinuities are not suitable for the model validation in multicomponent flows. The capability of handling strong shocks and weak post-shock contact discontinuities is more critical to the demonstration of any model for compressible multicomponent or multifluid flows.

AMS: Applied and numerical mathematics; Compressible fluids and gas dynamics

Keywords: Multicomponent flow; Contact discontinuities; Material interfaces; Interface capturing method; Godunov scheme; Shock-interface interaction; Fully conservative approach; Compressible flow; Numerical uncertainty analysis; Strong shock waves

1. Introduction

The numerical simulation of multicomponent or multifluid flows has received a great deal of attention during the past two decades because of its relevance to nuclear power reactor safety analyses, and more recently fusion technology developments. Other important research areas and main applications for multifluid flow simulations exist in aerospace engineering, chemical engineering, materials processing, internal combustion engines, and petroleum industry.

Several kinds of numerical methods with different physical models have been presented in the literature for the simulation of multifluid flows associated with contact discontinuities and shock waves. In this paper, we are particularly interested in the numerical solutions of hyperbolic conservation laws for the description of multicomponent non-reacting flows. It was motivated by our experimental work on the thermal and hydrodynamic issues related to inertial confinement fusion (ICF) performed at the Wisconsin Shock Tube Laboratory [5]. It has been recognized that high resolution and numerical stability can be achieved with reasonable accuracy in the numerical solutions of hyperbolic conservation laws by many numerical methods. In practice, it has been proven that this is true for the simulation of single-phase, single-fluid flows with strong shocks by Godunov-type and higher-order schemes or other methods, but that may not be the case for more complicated flows. For example, consider the numerical simulation of multifluid flows associated with contact discontinuities and shock waves. An extended conservative system of governing equations is widely used in which additional conservation equations are introduced to the original Euler equations to describe the conservation of some parameters like the mass fractions of each component and the ratio of specific heats of the mixture. This kind of extended conservation system of governing equations has been widely solved by many different numerical schemes during the past two decades. In the present work, it was found that the solution to this extended system of governing equations in conservative form, with the conventional "gamma" and "thermodynamic" models, often fails to maintain pressure equilibrium and results in oscillations and other computational inaccuracies near material interfaces [1,7,10,28–33] for example. It is important to note that these oscillations are not the ones commonly associated with high-order numerical methods and not observed in the single-fluid model either [3].

Numerous efforts have been made to overcome this kind of difficulty. A modification of the numerical flux was introduced by Larrouturou [32] to guarantee the positivity of mass fractions under a CFL-like condition. This modification does not prevent spurious oscillations of the solutions [7,32]. Karni [30] introduced a non-conservative scheme to capture the contact discontinuities using an additional non-conservative

governing equation for the evolution of the pressure. This approach is the first step toward understanding this complex problem with reduced conservation errors and reasonable results are obtained; however, it was unable to handle strong shocks due to the intrinsic drawbacks of the non-conservative schemes [2]. In some cases, the conservation errors become so large that the solution no longer converges to the right one [28]. Another significant effort is that presented by Abgrall [2]: a quasi-conservative approach for the simulation of multicomponent flows. In his approach, the density of each component has its own governing equation for preserving positive mass fraction and a non-conservative formulation for the ratio of specific heats of the mixture has been introduced. Although it is a quasi-conservative approach, reasonable results are obtained even for the case with strong shocks. But from Abgrall's [2] test case with a strong shock, we note that the overshoot of the velocity and undershoot of the density with the second-order numerical scheme are still visible. He also indicated that this approach might not be applicable with certain numerical schemes like the van Leer. Recently, Shyue [52] extended Abgrall's idea to the simulation of multifluid flows with the so-called "stiffened" gas equation of state and in multiple dimensions, and reasonable results are obtained. Saurel and Abgrall [48] had presented a similar scheme at the same time. More recently, Shyue [53] extended this kind of quasi-conservative approach to the simulation of multifluid flows with a van der Waals equation of state and further with a Mie–Gruneisen equation of state [54]. Saurel and Abgrall [49] also presented a multiphase Godunov method for compressible multifluid and multiphase flows. We have just learned that the authors of [4] developed a five-equation model for the simulation of interfaces between compressible fluids with general equations of state. Actually, this model is an extension of the quasi-conservative approach to a general EOS by using more additional equations for densities and volume fractions, associated with a compromise between the original quasi-conservative mixture model [2] and the quasi-conservative two-fluid model [49].

There are many other numerical methods available in the literature for the simulation of multicomponent or multifluid flows. Some typical ones are front-tracking methods [8,11,12,16,22,26,34,36,37], level-set methods [6,18,40], volume-of-fluid methods [15,39,56] ([15] was cited therein [52]), BKG-based methods [66], and more recently, the ghost-fluid-method [20], and ghost-fluid-method-like method [35]. See [3,48,50] for a good, concise review of the up-to-date mathematical models and numerical methods for the simulation of multicomponent or multifluid flows.

Despite considerable efforts during the past two decades, a thermodynamically consistent and fully conservative description of multicomponent flows with shock-interface interactions is still missing. Moreover, the development of both non-conservative [30] and quasi-conservative [2] approaches is based upon a claim that the conservative form of the governing equations is the main reason why conventional conservative approaches fail to obtain oscillation-free solutions for multifluid flows and that one must abandon the strict "conservative form" requirement. One more fact can be seen is surprising that almost all of later efforts [3,4,31,48–50,52–54] have been made in the field following a path of the non-conservative and quasi-conservative approaches by Karni [30] and Abgrall [2] but the conservative approaches have been disregarded for years. These facts have made us interested to find out what is the real reason why the conventional conservative approaches have been disregarded by the researchers and further to seek for the possibility of developing a thermodynamically consistent and fully conservative approach. Our analysis shows instead that there is nothing wrong with the conservative form of the governing equations in conventional approaches and that the main problem is that the formulation or the governing equation used for the determination of the ratio of specific heats is inappropriate. In the past, improved results could be obtained in the simulation of multicomponent flows with non-conservative or quasi-conservative approaches only because different ways were used to compute the pressure or the ratio of specific heats of the mixture near interfaces. Our new, fully conservative model will support this point.

Our goal is to propose a simple and fully conservative model for the best description of multicomponent or multifluid flows. The model should be physically consistent, fully conservative, independently of the type

of numerical scheme used to implement it, and should generate oscillation-free solutions near material interfaces. The development of our model is based upon the very simple and physically sound concept that the total energy of the mixture should be conserved at any time. Starting from the conservation equation governing the total energy of the mixture in terms of the total enthalpy, we obtain a new formulation for the determination of the ratio of specific heats of the mixture. During this process, we also obtain a conservative-form equation to govern the pressure. Another formulation is derived to determine the molecular weight of the mixture from classical thermodynamics. The governing equations are further derived to calculate the specific heat ratio and the molecular weight of the mixture with their new formulations and the continuity or mass fraction equations for the individual components. These three conservative-form equations for the ratio of specific heats, the molecular weight and the pressure, combined with the other two conservative-form equations governing mass and momentum, offer a new, fully conservative system of governing equations that can be used for the description of multicomponent or multifluid flows and that can be solved using any kind of numerical schemes.

Since our focus in this paper is on the development of a new conservative system for the simulation of multicomponent flows, the numerical method used for the solution of the model equations is not so important. Although any kind of numerical schemes applicable for the solution of hyperbolic laws (for example [13,27,34,41,43–45,59,60,62]) can be used, here we present a Godunov-type method based upon a fast exact Riemann solver to solve our proposed system of governing equations. We choose a Godunov-type scheme because it always captures the locations of strong shock waves correctly even it is only first-order accurate. We use Pike's [42] solver that seems to be one of the fastest exact Riemann solvers available to date in the literature. To improve the accuracy of the scheme, we use the MUSCL (monotone upstream-centered scheme for conservation laws) technique for the data reconstruction of fluxes. We will briefly describe this solver in Section 3.

The outline of this paper is as follows. In Section 2, two conventional and representative extensions of the single component Euler's equation to multicomponent flows are described. In Section 3, based upon the concept of total energy conservation for the mixture, we derive our thermodynamically consistent and fully conservative (TCFC) model that involves two new formulations for the calculation of the ratio of specific heats and the molecular weight of the mixture and three conservative-form equations for them and the pressure. Also, a simple version of the model is developed from its general form without solving the governing equation for the molecular weight of the mixture. A brief description is further given in this section about the numerical uncertainty analysis and why the conventional conservation models are inconsistent. A brief analysis of the proposed TCFC models and conventional conservative models is also presented in this section on the evolution of the pressure field across material fronts for a mixture associated with isolated contact discontinuities. In Section 4, we briefly describe our solver, developed for solving the governing equations of proposed new model and conventional models. Four test cases of multicomponent flows with both strong and weak shocks are simulated using the proposed new fully conservative model and conventional conservative models and the results are presented in Section 5. The numerical results, their analyses and the comparison with results obtained with conventional fully conservative models as well as exact solutions (when possible) are also presented in this section. In Section 6 the important conclusions of this paper are summarized.

2. Conventional conservation models

In this paper, we are interested in the simulation of multicomponent, non-reacting flow without viscosity, heat transfer and gravity. For brevity and without loss of generality, the following discussion is specialized, but not limited, to two component flows.

The single-component continuity, momentum and energy equations of gas dynamics have the form

$$\frac{\partial \rho}{\partial t} + \nabla \cdot (\rho \mathbf{V}) = 0, \tag{1}$$

$$\frac{\partial (\rho \mathbf{V})}{\partial t} + \nabla \cdot (\rho \mathbf{V} \otimes \mathbf{V} + p\mathbf{I}) = 0, \tag{2}$$

$$\frac{\partial E}{\partial t} + \nabla \cdot [(E + p)\mathbf{V}] = 0, \tag{3}$$

where ρ, p and E denote density, pressure and total energy per unit volume, respectively, $\mathbf{V}$ and $\mathbf{I}$ are the velocity vector and the unit tensor, respectively, and we use $H = (E + p)/\rho$ to denote total enthalpy per unit mass. For ideal gases, the equation of state is

$$e = \frac{p}{\rho(\gamma - 1)} \tag{4}$$

with $E = \rho(e + \mathbf{V}^2/2)$. Here γ is the ratio of specific heats and e is the internal energy per unit mass. We will use Eqs. (1)–(3) with equation of state (4) as model equations in the following discussions.

We now discuss extensions of the aforementioned single component Euler-type governing equations to the two-component case. We assume that the gas is a mixture of two calorically perfect gases and that the pressure is determined using Dalton's law. In a common approach, the two components are assumed to have the same flow variables like pressure, velocity, and temperature in one computational cell but different properties like microscopic density and γ. Under these assumptions, the governing equations for single component flows can be used directly for the description of multicomponent flows if γ of the mixture is known. There are two typical ways, in conventional conservative approaches, to calculate γ for the mixture. One is based upon the mass fractions of the components and some thermodynamic relationships. The mass fractions of the components can be calculated from their governing equations derived from the continuity equations for the mixture and the components. The governing equations for the mass fractions of the components have the following conservative form (e.g. [32])

$$\frac{\partial (\rho Y_i)}{\partial t} + \nabla \cdot (\rho \mathbf{V} Y_i) = 0, \tag{5}$$

where Y_i is the mass fraction of the ith component (i is either 1 or 2 for a two-component flow). Note that only $i - 1$ equations are independent for the calculation of the mass fractions although each component has its own equation because the sum of all mass fractions must be unity. Here we also note that the volume fractions are equivalent to the mole fractions. For a two-component fluid, this leads to a formulation for the calculation of the value of γ from classical thermodynamics as below (e.g. [30,32])

$$\gamma = \frac{Y_1 C_{v1} \gamma_1 + Y_2 C_{v2} \gamma_2}{Y_1 C_{v1} + Y_2 C_{v2}}, \tag{6}$$

where C_{v1} and C_{v2} are the specific heats (at constant volume) of component 1 and 2, respectively. We can also use an alternative form of Eq. (6) to avoid using the specific heats, as below [63]

$$\gamma = \frac{Y_1 \gamma_1 M_2 (\gamma_2 - 1) + Y_2 \gamma_2 M_1 (\gamma_1 - 1)}{Y_1 M_2 (\gamma_2 - 1) + Y_2 M_1 (\gamma_1 - 1)}, \tag{7}$$

where M_1, M_2 are the molecular weights of the two components, respectively. Eq. (7) is equivalent to Eq. (6).

Another approach to calculate γ is to solve a governing equation for it directly instead of using the mass fractions and thermodynamic relationships. The equation governing γ in conservative form is (e.g. [30,32,46]) ([46] was cited therein [30])

$$\frac{\partial(\rho\gamma)}{\partial t} + \nabla \cdot (\rho \mathbf{V}\gamma) = 0, \tag{8}$$

where γ is locally calculated from the quotient $\gamma = (\rho\gamma)/(\rho)$ after having solved Eq. (8).

Now we can summarize two typical conventional extended Euler models considered in this paper as:

1. *''Thermodynamic'' model* (e.g. [1,30,32]). The set of Eqs. (1)–(3), (5), and (6) or (7) offer a conventional conservation model for the simulation of multicomponent flows. This approach is designated as the ''thermodynamic'' model in this paper as the calculation of γ for the mixture involves Eq. (6) or (7) which are derived from classical thermodynamics.
2. *''Gamma'' model* (e.g. [1,30,32,46]). The set of Eqs. (1)–(3), and (8) give another conventional conservation model for the description of multicomponent flows. This approach is designated as the ''gamma'' model in this paper since the value of γ for the mixture is determined directly from its governing transport Eq. (8).

It should be mentioned that in both ''thermodynamic'' and ''gamma'' models, the pressure is calculated by using Eq. (4).

3. New fully conservative approach (TCFC model)

Two typical extensions of the single-component Euler equations to the description of a multicomponent flow have been described in the previous section. Unfortunately, these two typical conservative approaches often fail to maintain pressure equilibrium and result in oscillations and other computational inaccuracies near material interfaces. In this section, we first present the derivation of the general thermodynamically consistent and fully conservative model (TCFC model) for the description of multicomponent flows. A simple version of the TCFC model is given next. The non-conservative form of the additional formulations in the TCFC models is also discussed. The numerical uncertainty analysis of the proposed TCFC models, conventional conservative ''thermodynamic'' and ''gamma'' models is then presented. A brief analysis of the proposed TCFC models and the conventional conservative models is finally given on the pressure evolution across material fronts for a mixture associated with isolated contact discontinuities.

3.1. The general TCFC model

We now derive a general TCFC model for the description of multicomponent flows based upon multiphase fluid dynamics. Our starting point is that the total energy of the mixture should be conserved at any time. From multiphase fluid dynamics, we have the conservative-form governing equations for the total energy of a mixture of ideal gases in terms of enthalpy, without viscosity and chemical reactions, shown as below:

$$\frac{\partial}{\partial t}\left[\alpha_1\rho_1\left(h_1 + \frac{1}{2}\mathbf{V}_1^2\right)\right] + \nabla \cdot \left[\alpha_1\rho_1\left(h_1 + \frac{1}{2}\mathbf{V}_1^2\right)\mathbf{V}_1\right] - \alpha_1\frac{\partial p_1}{\partial t} = 0 \tag{9}$$

for component 1 (or fluid 1) and

$$\frac{\partial}{\partial t}\left[\alpha_2\rho_2\left(h_2 + \frac{1}{2}\mathbf{V}_2^2\right)\right] + \nabla \cdot \left[\alpha_2\rho_2\left(h_2 + \frac{1}{2}\mathbf{V}_2^2\right)\mathbf{V}_2\right] - \alpha_2\frac{\partial p_2}{\partial t} = 0 \tag{10}$$

for component 2 (or fluid 2), where α is the volume fraction of each component, and h is the enthalpy per unit mass of each component, determined by

$$h = e + \frac{p}{\rho}. \tag{11}$$

From the sum of Eqs. (9) and (10), we can obtain the conservative form of the equation governing the total enthalpy of the mixture as

$$\frac{\partial}{\partial t}\left[\alpha_1\rho_1\left(h_1 + \frac{1}{2}\mathbf{V}_1^2\right) + \alpha_2\rho_2\left(h_2 + \frac{1}{2}\mathbf{V}_2^2\right)\right] + \nabla\cdot\left[\alpha_1\rho_1\left(h_1 + \frac{1}{2}\mathbf{V}_1^2\right)\mathbf{V}_1 + \alpha_2\rho_2\left(h_2 + \frac{1}{2}\mathbf{V}_2^2\right)\mathbf{V}_2\right] - \left(\alpha_1\frac{\partial p_1}{\partial t} + \alpha_2\frac{\partial p_2}{\partial t}\right) = 0. \tag{12}$$

As stated before, here we assume that each component has the same state variables (pressure, velocity and temperature) as the mixture. We can now simplify Eq. (12) as follows:

$$\frac{\partial}{\partial t}\left[(\alpha_1\rho_1 h_1 + \alpha_2\rho_2 h_2) + \frac{1}{2}(\alpha_1\rho_1 + \alpha_2\rho_2)\mathbf{V}^2\right] + \nabla\cdot\left[\left((\alpha_1\rho_1 h_1 + \alpha_2\rho_2 h_2) + \frac{1}{2}(\alpha_1\rho_1 + \alpha_2\rho_2)\mathbf{V}^2\right)\mathbf{V}\right] - \frac{\partial p}{\partial t} = 0. \tag{13}$$

Substituting the equation of state (4) and Eq. (11) into the above equation, we have

$$\frac{\partial}{\partial t}\left[\left(\frac{\alpha_1\gamma_1}{\gamma_1 - 1} + \frac{\alpha_2\gamma_2}{\gamma_2 - 1}\right)p + \frac{1}{2}\rho\mathbf{V}^2\right] + \nabla\cdot\left[\left(\left(\frac{\alpha_1\gamma_1}{\gamma_1 - 1} + \frac{\alpha_2\gamma_2}{\gamma_2 - 1}\right)p + \frac{1}{2}\rho\mathbf{V}^2\right)\mathbf{V}\right] - \frac{\partial p}{\partial t} = 0, \tag{14}$$

where $\rho = \alpha_1\rho_1 + \alpha_2\rho_2$ is the density of the mixture. It is interesting to look at the form of Eq. (14): the total energy conservation equation for the mixture takes the same form as that for a single component if and only if we define

$$\chi = \frac{\gamma}{\gamma - 1} = \frac{\alpha_1\gamma_1}{\gamma_1 - 1} + \frac{\alpha_2\gamma_2}{\gamma_2 - 1} = \alpha_1\chi_1 + \alpha_2\chi_2, \tag{15}$$

where γ is the ratio of specific heats of the mixture, γ_1, γ_2 are the ratios of specific heats of the individual components, and χ is an additional parameter introduced to simplify the expression of the governing equations. We note that χ is actually the ratio of the specific heat at constant pressure to the gas constant, $\chi \equiv C_p/R$. Substituting χ into Eq. (14), we can rewrite the latter in a simple form as

$$\frac{\partial}{\partial t}\left[(\chi - 1)p + \frac{1}{2}\rho\mathbf{V}^2\right] + \nabla\cdot\left[\left(\chi p + \frac{1}{2}\rho\mathbf{V}^2\right)\mathbf{V}\right] = 0. \tag{16}$$

Eq. (16) is the simplified total energy conservation equation for the mixture that can be used to calculate the pressure with the quotient $p = (((\chi - 1)p + 1/2\rho\mathbf{V}^2) - 1/2\rho\mathbf{V}^2)/(\chi - 1)$. We note that the pressure term in Eq. (14) has been included in the first term in Eq. (16) for the convenience of real calculations.

Our next concern is how to calculate the mixture parameter χ. From classical thermodynamics, it is known that the volume fractions are equivalent to the mole fractions based upon the above assumptions

$$\alpha_1 = \frac{n_1}{n}, \quad \alpha_2 = \frac{n_2}{n}, \tag{17}$$

where n_1 and n_2 are the mole numbers for component 1 and 2, respectively, and $n = n_1 + n_2$ is the total number of moles of the mixture. We also have

$$n_1 = \frac{m_1}{M_1}, \quad n_2 = \frac{m_2}{M_2}, \quad n = \frac{m}{M}, \tag{18}$$

where m_1, m_2 and m are the masses of component 1, 2 and the mixture, respectively. From Eqs. (15), (17) and (18), we obtain

$$\frac{m}{M}\chi = \frac{m_1}{M_1}\chi_1 + \frac{m_2}{M_2}\chi_2. \tag{19}$$

Furthermore, according to the relationships between the masses and densities in a control volume V,

$$m_1 = \alpha_1\rho_1, \quad m_2 = \alpha_2\rho_2 V, \quad m = \alpha\rho V, \tag{20}$$

and with Eq. (19), we have

$$\frac{\chi}{M}\rho = \frac{\chi_1}{M_1}(\alpha_1\rho_1) + \frac{\chi_2}{M_2}(\alpha_2\rho_2). \tag{21}$$

Multiplying both sides of Eq. (21) by the velocity vector of the mixture we obtain

$$\frac{\chi}{M}\rho\mathbf{V} = \frac{\chi_1}{M_1}(\alpha_1\rho_1\mathbf{V}) + \frac{\chi_2}{M_2}(\alpha_2\rho_2\mathbf{V}). \tag{22}$$

Taking the derivative of Eq. (21) with respect to time and the divergence of Eq. (22), we have

$$\frac{\partial}{\partial t}\left(\frac{\chi}{M}\rho\right) = \frac{\partial}{\partial t}\left[\frac{\chi_1}{M_1}(\alpha_1\rho_1)\right] + \frac{\partial}{\partial t}\left[\frac{\chi_2}{M_2}(\alpha_2\rho_2)\right] \tag{23}$$

and

$$\nabla\cdot\left(\frac{\chi}{M}\rho\mathbf{V}\right) = \nabla\cdot\left[\frac{\chi_1}{M_1}(\alpha_1\rho_1\mathbf{V})\right] + \nabla\cdot\left[\frac{\chi_2}{M_2}(\alpha_2\rho_2\mathbf{V})\right]. \tag{24}$$

Adding Eqs. (23) and (24) and noting that χ_1, χ_2, M_1 and M_2 are constants, we obtain

$$\frac{\partial}{\partial t}\left(\frac{\chi}{M}\rho\right) + \nabla\cdot\left(\frac{\chi}{M}\rho\mathbf{V}\right) = \frac{\chi_1}{M_1}\left[\frac{\partial}{\partial t}(\alpha_1\rho_1) + \nabla\cdot(\alpha_1\rho_1\mathbf{V})\right] + \frac{\chi_2}{M_2}\left[\frac{\partial}{\partial t}(\alpha_2\rho_2) + \nabla\cdot(\alpha_2\rho_2\mathbf{V})\right]. \tag{25}$$

Applying conservation of mass for each component to Eq. (25), it is seen that both of the terms in square brackets are zero, therefore,

$$\frac{\partial}{\partial t}\left(\frac{\chi}{M}\rho\right) + \nabla\cdot\left(\frac{\chi}{M}\rho\mathbf{V}\right) = 0. \tag{26}$$

Eq. (26) provides the closure equation to calculate the parameter χ. For a complete solution, we need the molecular weight of the mixture M. From classical thermodynamics, we have

$$\frac{1}{M} = \frac{n}{m} = \frac{n_1 + n_2}{m}. \tag{27}$$

Using Eq. (18), we obtain

$$\frac{1}{M} = \frac{m_1/m}{M_1} + \frac{m_2/m}{M_2} = \frac{Y_1}{M_1} + \frac{Y_2}{M_2}. \tag{28}$$

Similar to the derivation of Eq. (26), if we multiply both sides of Eq. (28) by the density and momentum of the mixture, we have

$$\frac{1}{M}\rho = \frac{Y_1\rho}{M_1} + \frac{Y_2\rho}{M_2} \tag{29}$$

and

$$\frac{1}{M}\rho\mathbf{V} = \frac{Y_1\rho\mathbf{V}}{M_1} + \frac{Y_2\rho\mathbf{V}}{M_2}. \tag{30}$$

Taking the derivative of Eq. (29) with respect to time and the divergence of Eq. (30), we obtain

$$\frac{\partial}{\partial t}\left(\frac{1}{M}\rho\right) = \frac{\partial}{\partial t}\left(\frac{Y_1\rho}{M_1}\right) + \frac{\partial}{\partial t}\left(\frac{Y_2\rho}{M_2}\right) \tag{31}$$

and

$$\nabla\cdot\left(\frac{1}{M}\rho\mathbf{V}\right) = \nabla\cdot\left(\frac{Y_1\rho\mathbf{V}}{M_1}\right) + \nabla\cdot\left(\frac{Y_2\rho\mathbf{V}}{M_2}\right). \tag{32}$$

Adding Eqs. (31) and (32), and noting that M_1 and M_2 are constants, we have

$$\frac{\partial}{\partial t}\left(\frac{1}{M}\rho\right) + \nabla\cdot\left(\frac{1}{M}\rho\mathbf{V}\right) = \frac{1}{M_1}\left[\frac{\partial}{\partial t}(Y_1\rho) + \nabla\cdot(Y_1\rho\mathbf{V})\right] + \frac{1}{M_2}\left[\frac{\partial}{\partial t}(Y_2\rho) + \nabla\cdot(Y_2\rho\mathbf{V})\right]. \tag{33}$$

In Eq. (33), the terms inside the square brackets are the mass fraction balance terms for each of the two components, respectively: hence, both square brackets are again equal to zero, therefore

$$\frac{\partial}{\partial t}\left(\frac{1}{M}\rho\right) + \nabla\cdot\left(\frac{1}{M}\rho\mathbf{V}\right) = 0. \tag{34}$$

Eq. (34) gives an equation for $1/M$, and the parameter χ can be calculated by the quotient

$$\chi = \frac{(\chi/M)}{(1/M)}. \tag{35}$$

The set of Eqs. (1), (2), (16), (26) and (34) offer the new hyperbolic conservation laws for the description of compressible multicomponent flows associated with contact discontinuities and shock waves. Then the ratio of specific heats of the mixture can be calculated after computing the value χ from Eq. (35) as below

$$\gamma = \frac{\chi}{\chi - 1}. \tag{36}$$

The volume fractions can then be calculated directly by using

$$\alpha_1 = \frac{\chi - \chi_2}{\chi_1 - \chi_2}, \quad \alpha_2 = 1 - \alpha_1, \tag{37}$$

or

$$\alpha_2 = \frac{\chi - \chi_1}{\chi_2 - \chi_1}, \quad \alpha_1 = 1 - \alpha_2. \tag{38}$$

Similarly, the mass fractions can also be obtained, without solving their governing equations like in the conventional conservative, non-conservative and quasi-conservative approaches, by

$$Y_1 = \frac{1/M - 1/M_2}{1/M_1 - 1/M_2}, \quad Y_2 = 1 - Y_1, \tag{39}$$

or

$$Y_2 = \frac{1/M - 1/M_1}{1/M_2 - 1/M_1}, \quad Y_1 = 1 - Y_2. \tag{40}$$

3.2. A simple version of the TCFC model

If knowledge of the mass fractions and molecular weight of the mixture is not required, a useful alternative formulation of the model is as follows: from Eq. (34), using basic differential analysis, we have

$$\rho\left[\frac{\partial}{\partial t}\left(\frac{1}{M}\right) + \mathbf{V}\cdot\nabla\left(\frac{1}{M}\right)\right] + \frac{1}{M}\left[\frac{\partial}{\partial t}(\rho) + \nabla\cdot(\rho\mathbf{V})\right] = 0. \tag{41}$$

In Eq. (41), the term inside the second bracket is the mass balance term for the mixture: hence, the second square bracket is equal to zero, therefore we obtain

$$\frac{\partial}{\partial t}\left(\frac{1}{M}\right) + \mathbf{V}\cdot\nabla\left(\frac{1}{M}\right) = 0. \tag{42}$$

Similarly, from Eq. (26) we have

$$\frac{1}{M}\left[\frac{\partial}{\partial t}(\chi\rho) + \nabla\cdot(\chi\rho\mathbf{V})\right] + \chi\rho\left[\frac{\partial}{\partial t}\left(\frac{1}{M}\right) + \mathbf{V}\cdot\nabla\left(\frac{1}{M}\right)\right] = 0 \tag{43}$$

which, because of Eq. (42), reduces to

$$\frac{\partial}{\partial t}(\chi\rho) + \nabla\cdot(\chi\rho\mathbf{V}) = 0. \tag{44}$$

The set of Eqs. (1), (2), (16) and (44) provides a new, much simpler, fully conservative approach for the description of compressible multicomponent flows associated with contact discontinuities and shock waves and without adding new variables to the original system. This simple model can be used if the mass fractions are not required. Calculation of the volume fractions and γ can be performed as that in the general TCFC model using Eqs. (37) or (38) and (36), respectively.

Actually, we also found that the mass fractions can be calculated even without solving the governing equation for the molecular weight of the mixture like that in the general TCFC model. From Eqs. (17) and (18), we can obtain

$$Y_1 = \frac{\alpha_1 M_1}{\alpha_1 M_1 + \alpha_2 M_2}, \quad Y_2 = 1 - Y_1 \tag{45}$$

or

$$Y_2 = \frac{\alpha_2 M_2}{\alpha_1 M_1 + \alpha_2 M_2}, \quad Y_1 = 1 - Y_2. \tag{46}$$

Given the molecular weights of the individual components, the mass fractions can then be calculated by Eq. (45) or (46) after the volume fractions are determined by Eq. (37) or (38). Since the simple version of the

TCFC model is equivalent to the general form but much simpler, we suggest that the simple TCFC model be considered as the first choice for the description of multicomponent flow.

3.3. Non-conservative form of the additional formulations in the TCFC models

It is interesting to look at the relationship between the conservative form and the non-conservative form of the additional formulations in the TCFC models. Here we discuss Eq. (44) that governs the parameter χ of the mixture, as an example. Using some basic differential analysis, Eq. (44) can be rewritten as

$$\frac{\partial}{\partial t}(\chi\rho) + \nabla\cdot(\chi\rho\mathbf{V}) = \rho\left(\frac{\partial\chi}{\partial t} + \mathbf{V}\cdot\nabla\chi\right) + \chi\left(\frac{\partial\rho}{\partial t} + \nabla\cdot(\rho\mathbf{V})\right) = 0. \tag{47}$$

Considering the mass balance (1), Eq. (47) reduces to

$$\frac{\partial\chi}{\partial t} + \mathbf{V}\cdot\nabla\chi = 0. \tag{48}$$

Eq. (48) is the non-conservative form of Eq. (44) governing parameter χ for the mixture. It can be seen that Eq. (44) is analytically equivalent to Eq. (48) if the mass balance of the mixture (i.e. Eq. (1)) is satisfied. This implies that either conservative form (44) or non-conservative form (48) of χ equation can be used with other governing equations (in conservative form). Mathematically, this equivalence between the conservative form and the non-conservative form holds analytically. In discrete form, however, these two expressions may not be equivalent, as this depends on whether the product rule for differentiation used in Eq. (47) holds numerically. For example, from the numerical point of view, the conclusion on the equivalence between conservative and non-conservative forms becomes questionable in some case such as problems with strong shock waves. In general, conservative forms of the governing equations for χ and mass balance of the mixture can be well satisfied even if in the case of strong shock waves. That means, using Eqs. (1) and (44) implies the satisfaction of the non-conservative form of χ equation (with Eq. (47)). But on the other hand, the non-conservative form of χ equation is very difficult to be well satisfied in the case of strong shock waves due to the intrinsic limitations of non-conservative forms of governing equations. This means that using non-conservative form of χ equation with mass balance (1) does not always imply the satisfaction of the conservative form of χ equation, as it should do. For this reason, we suggest that one better to use the conservative forms of the additional formulations to ensure the best description of multicomponent flows associated with strong shock waves.

3.4. Analysis of numerical uncertainties of conventional conservative models

The TCFC models have been derived based upon multiphase fluid dynamics and classical thermodynamics. In this section, we present a brief analysis of the numerical uncertainties of conventional conservative models and the proposed TCFC model for the simulation of multicomponent flows.

From the computational fluid dynamics (CFD) point of view, numerical uncertainties (or errors) of the solution of any mathematically well-defined problem mainly come from two parts: the mathematical model and the numerical method both play important roles in the solution of a given flow problem [61]. A well-defined mathematical model consists of three parts: the governing equations, the initial conditions and the boundary conditions. On the other hand, a well-developed method for solving a well-defined mathematical model also consists of three parts: the numerical scheme for the discretization of the governing equations and the corresponding solution method for the discretized equations, the additional numerical boundary conditions, and the grid system. In the past two decades, a great deal of experience has shown that the numerical method is not the cause of solution-oscillations through material interfaces

in the simulation of multicomponent flows with conventional conservative approaches using different numerical schemes. Also, the test problems used in the past for the validations of conventional conservative approaches are classical Riemann problems in which the initial and boundary conditions are well defined. Hence, the main source of numerical uncertainties in the conventional conservative models for the simulation of multicomponent flows could be the governing equations, particularly the additional formulations and governing equations used for the calculation of the mass fractions and the ratio of specific heats of the mixture.

Any equations (like the equations for the mass fractions, γ-value etc) added to the original conservation equations (mass, momentum, energy) must be consistent with these latter. Let us discuss the proposed TCFC model first: the new formulation (15) is consistent with the original governing equations for the mixture. Substituting (15) into (16) with the definition of density for the mixture, we can revert to the initial Eq. (12) governing the total energy balance for the mixture in terms of enthalpy. Also, it is easily shown that formulation (15) is equivalent to formulation (6) or (7) which was derived from classical thermodynamics. Furthermore, the derivation of additional Eqs. (26) and (34) for the general form (or Eq. (44) for the simple version) of the TCFC model is logically and physically reasonable, and only the mass balance and mass fractions balance equations for the individual components are used during the process. That means that the continuity equations and mass fractions equations for the individual components are implicitly and accurately satisfied when the additional Eqs. (26) and (34) (or Eq. (44) for the simple version) are added to the original system in the TCFC models. So formulations (15) and (28) and their corresponding governing Eqs. (26) and (34) (Eq. (44) for the simple version) in conservative form are thermodynamically consistent with the original governing equations for the description of multicomponent flow. Therefore, the proposed approaches are really TCFC models.

A similar analysis applies to the conventional conservative ''gamma'' model, which is actually equivalent to the ''thermodynamic'' model implemented using a linear interpolation technique for the definition of γ. Using the same strategy, if we substitute a linear interpolation formulation for the ratio of specific heats into the energy equation we see that Eq. (16) cannot be reverted to the initial Eq. (12) governing the total energy balance for the mixture in terms of the enthalpy. Actually, a linear interpolation for the determination of the ratio of specific heats for the mixture cannot be thermodynamically consistent as the formulations (6), (7) or (15) provide different forms of thermodynamically consistent definitions based upon classical thermodynamics, all of which are non-linear. So the conventional conservative ''gamma'' model is thermodynamically inconsistent with the original governing equations.

Our next concern is about the conventional conservative ''thermodynamic'' model. We have already shown that Eqs. (6), (7) for the ratio of specific heats are thermodynamically consistent with the original system since they were derived from classical thermodynamics. But the calculation of γ based upon (6) or (7) and the mass fractions may not be appropriate because the calculation is indirectly performed in a different time loop from other solved variables. Here we briefly discuss why the indirect calculation of the ratio of specific heats is inappropriate in the conventional conservative ''thermodynamic'' model. Let us define the truncation errors of the mass balance equations for the individual components and the mixture, and Eq. (26) for the mixture parameter χ/M after their discretizations as

$$\begin{aligned}
\Delta m_1 &= L(m_1) - L_\Delta(m_1),\\
\Delta m_2 &= L(m_2) - L_\Delta(m_2),\\
\Delta m_m &= L(m_m) - L_\Delta(m_m),\\
\Delta m_{\chi/M} &= L\left(m_{\chi/M}\right) - L_\Delta\left(m_{\chi/M}\right),
\end{aligned} \tag{49}$$

where L, L_Δ are the differential and finite-difference operators, respectively, and $m_1, m_2, m_m, m_{\chi/M}$ stand for the mass balance equations for the individual components, the mixture and the governing equation for χ/M, respectively. From Eqs. (25) and (49), we have

$$\Delta m_{\chi/M} = \frac{\chi_2}{M_2}\Delta m_m + \left(\frac{\chi_1}{M_1} - \frac{\chi_2}{M_2}\right)\Delta m_1 \quad \text{or}$$
$$\Delta m_{\chi/M} = \frac{\chi_1}{M_1}\Delta m_m + \left(\frac{\chi_2}{M_2} - \frac{\chi_1}{M_1}\right)\Delta m_2. \tag{50}$$

From Eq. (50), we see that Eq. (26) would be satisfied under two conditions. One case is that the mass balance equations for both the mixture and one of the individual components are exactly satisfied. Another one is that both individual components have the same value of the ratio of specific heats and the molecular weights (similar gases): in such case the truncation error for Eq. (26) has the same value as that of the mass balance equation for the mixture. But in the real case, it would be very difficult to meet these two conditions. Similarly, if we define the truncation errors of the mass fraction balance equations for the individual components and Eq. (34) for the molecular weight after their discretizations as

$$\begin{aligned}
\Delta m_{Y_1} &= L(m_{Y_1}) - L_\Delta(m_{Y_1}),\\
\Delta m_{Y_2} &= L(m_{Y_2}) - L_\Delta(m_{Y_2}),\\
\Delta m_{1/M} &= L\left(m_{1/M}\right) - L_\Delta\left(m_{1/M}\right),
\end{aligned} \tag{51}$$

where $m_{Y_1}, m_{Y_2}, m_{1/M}$ stand for the mass fraction equations for the individual components and the governing Eq. (34) for $1/M$, respectively. From Eqs. (33) and (51), we have

$$\Delta m_{1/M} = \frac{1}{M_2}\Delta m_m + \left(\frac{1}{M_1} - \frac{1}{M_2}\right)\Delta m_{Y_1} \quad \text{or}$$
$$\Delta m_{1/M} = \frac{1}{M_1}\Delta m_m + \left(\frac{1}{M_2} - \frac{1}{M_1}\right)\Delta m_{Y_2}. \tag{52}$$

From Eq. (52), one can see that Eq. (34) would be satisfied under two conditions. Similar to the analysis of Eq. (50), one case is that the mass balance and mass fraction equations for both the mixture and one of the individual components are exactly satisfied. Another one is that both individual components have the same molecular weights (similar gases): in such case the truncation error for Eq. (34) has the same value as that of the mass balance equation for the mixture. But in the real case, it would also be very difficult to meet these two conditions. In summary, the calculation of γ involves mass balance and mass fractions for the mixture and the individual components. In the TCFC models (Eqs. (26), (34) and (35) for the general model, or Eq. (44) for the simple model), all of these mass balance and mass fraction equations are accurately and implicitly satisfied. But in the conventional "thermodynamic" model, the indirect calculation of the value of γ for the mixture of different gases, the truncation errors of the mass balance equations for the mixture (density calculation) and one individual component (also mass fraction calculation) are not exactly zero and could become very large in some case like that of strong shocks. These errors could be increasing with time for transient problems. In such case, the calculated value of γ for the mixture based on the mass fractions (indirect calculation) could not be satisfied with the Eqs. (26) and (34) (or (44)), as it should be. Therefore, the calculating procedure in the conventional conservative "thermodynamic" model is inappropriate for the determination of the ratio of specific heats of the mixture.

3.5. Evolution of the pressure field for isolated contact discontinuities

A brief analysis of the proposed TCFC models and the conventional conservative models has been given in the last sub-section from a general viewpoint of numerical uncertainty analysis. In this sub-section, we present a numerical analysis of the TCFC models on the evolution of the pressure field for a mixture associated with isolated contact discontinuities to ensure that the proposed TCFC models are able to simulate

the problem properly. A brief analysis of the conventional conservative models is given next and the pressure oscillation rates generated by the models are also estimated.

Our analysis is performed follow the lines by Abgrall and Karni [3]. Using $\delta(\,) = (\,)^{n+1} - (\,)^n$ to denote time changes, $\Delta(\,) = (\,)_{j+(1/2)} - (\,)_{j-(1/2)}$ spatial variations, and $v = \Delta t/\Delta x$ the mesh ratio, the Godunov scheme applied to the 1D case of the TCFC model (simple version, for example) gives

$$\begin{pmatrix} \rho \\ \rho u \\ \rho\chi \\ E \end{pmatrix}_j^{n+1} = \begin{pmatrix} \rho \\ \rho u \\ \rho\chi \\ E \end{pmatrix}_j^{n} + \begin{pmatrix} \delta(\rho) \\ \delta(\rho u) \\ \delta(\rho\chi) \\ \delta(E) \end{pmatrix}, \tag{53}$$

where superscript n denotes the time step, subscript j stands for the cell location, and

$$\begin{pmatrix} \delta(\rho) \\ \delta(\rho u) \\ \delta(\rho\chi) \\ \delta(E) \end{pmatrix} = -v \begin{pmatrix} \Delta(\rho u) \\ \Delta(\rho u^2 + p) \\ \Delta(\rho\chi u) \\ \Delta(u(\chi p + 1/2\rho u^2)) \end{pmatrix} \tag{54}$$

with

$$E = (\chi - 1)p + \frac{1}{2}\rho u^2. \tag{55}$$

Considering a flow consisting of a material interface separating two ideal gases with γ_{L} and γ_{R}, moving with some positive velocity $u > 0$, with initial data

$$W_j^0 = \begin{cases} \left(\rho, \rho u, \rho\chi_{\mathrm{L}}, (\chi_{\mathrm{L}} - 1)p + \frac{\rho}{2}u^2\right), & j < 1, \\ \left(\rho, \rho u, \rho\chi_{\mathrm{R}}, (\chi_{\mathrm{R}} - 1)p + \frac{\rho}{2}u^2\right), & j \geqslant 1. \end{cases} \tag{56}$$

In this case, the numerical flux reduces to the upwind flux,

$$F_{j+1/2} = F(W_j), \tag{57}$$

and after one time step, we have

$$W_1^1 = W_1^0 - v\left(F(W_1^0) - F(W_0^0)\right). \tag{58}$$

Using some simple algebra we can obtain that after one time step

$$\begin{aligned} \rho_1^1 &= \rho, \\ u_1^1 &= u, \\ \chi_1^1 &= vu\chi_{\mathrm{L}} + (1 - vu)\chi_{\mathrm{R}}, \\ E_1^1 &= (vu\chi_{\mathrm{L}} + (1 - vu)\chi_{\mathrm{R}} - 1)p + \frac{1}{2}\rho u^2. \end{aligned} \tag{59}$$

Substituting Eq. (59) into equation of state (55), with some rearrangements, we have

$$(vu\chi_{\mathrm{L}} + (1 - vu)\chi_{\mathrm{R}} - 1)(p_1^1 - p) = 0. \tag{60}$$

From Eq. (60) we can see that, if $0 < vu < 1$, the term $(vu\chi_{\mathrm{L}} + (1 - vu)\chi_{\mathrm{R}} - 1)$ will absolutely be non-zero. That implies that

$$p_1^1 = p. \tag{61}$$

Eq. (61) is the only solution satisfied with Eq. (60). That means the computed p_1^1 remains uniform across the material fronts, as it should be.

Here we also give an analysis of the conventional conservative gamma model and thermodynamic model on the pressure evolution for isolated contact discontinuities to support our conclusions obtained from a general viewpoint of numerical uncertainty analysis.

For the *thermodynamic model*, we have an additional equation for the computation of mass fractions as below

$$(\rho Y)_j^{n+1} = (\rho Y)_j^n + \delta(\rho Y), \tag{62}$$

where

$$\delta(\rho Y) = -v\Delta(\rho Y u). \tag{63}$$

Considering a similar flow problem consisting of a material interface separating two ideal gases with γ_L and γ_R, moving with some positive velocity $u > 0$, with initial data similar to Eq. (56)

$$W_j^0 = \begin{cases} \left(\rho, \rho u, \frac{1}{\gamma_L - 1} p + \frac{\rho}{2} u^2, \rho\right), & j < 1, \\ \left(\rho, \rho u, \frac{1}{\gamma_R - 1} p + \frac{\rho}{2} u^2, 0\right), & j \geqslant 1. \end{cases} \tag{64}$$

Following the same lines for the TCFC model as above, we have

$$\begin{aligned} &\rho_1^1 = \rho, \\ &u_1^1 = u, \\ &(Y_1)_1^1 = vu, \\ &(Y_2)_1^1 = 1 - vu, \\ &E_1^1 = \left(\frac{vu}{\gamma_L - 1} + \frac{1 - vu}{\gamma_R - 1}\right) p + \frac{1}{2}\rho u^2. \end{aligned} \tag{65}$$

Substituting the expression of E_1^1 in Eq. (65) into the equation of state (55) (in terms of γ) gives

$$\frac{p_1^1}{\gamma_1^1 - 1} = \left(\frac{vu}{\gamma_L - 1} + \frac{1 - vu}{\gamma_R - 1}\right) p. \tag{66}$$

Substituting the expressions of $(Y_1)_1^1$ and $(Y_2)_1^1$ in Eq. (65) into Eq. (7), we obtain

$$\begin{aligned} \frac{1}{\gamma_1^1 - 1} &= \frac{vuM_R(\gamma_R - 1) + (1 - vu)M_L(\gamma_L - 1)}{(\gamma_R - 1)(\gamma_L - 1)(vuM_R + (1 - vu)M_L)} \\ &= \frac{vu}{\gamma_L - 1} + \frac{1 - vu}{\gamma_R - 1} + \frac{vu(1 - vu)(M_R - M_L)(\gamma_R - \gamma_L)}{(\gamma_R - 1)(\gamma_L - 1)(vuM_R + (1 - vu)M_L)}. \end{aligned} \tag{67}$$

From Eqs. (66) and (67), we have

$$\left(\frac{vu}{\gamma_L - 1} + \frac{1 - vu}{\gamma_R - 1}\right) p_1^1 + \left(\frac{vu(1 - vu)(M_R - M_L)(\gamma_R - \gamma_L)}{(\gamma_R - 1)(\gamma_L - 1)(vuM_R + (1 - vu)M_L)}\right) p_1^1 = \left(\frac{vu}{\gamma_L - 1} + \frac{1 - vu}{\gamma_R - 1}\right) p. \tag{68}$$

Eq. (68) can be rewritten as

$$\frac{p_1^1 - p}{p_1^1} = -\frac{vu(1 - vu)(M_R - M_L)(\gamma_R - \gamma_L)}{(vuM_R + (1 - vu)M_L)(vu(\gamma_R - 1) + (1 - vu)(\gamma_L - 1))}. \tag{69}$$

If $0 < vu < 1$, from the above equation it can be seen that the newly computed pressure $p_1^1 \neq p$, therefore a pressure oscillation is generated. The oscillation rate has the value as that of the term at the right hand of Eq. (69) and has a definite sign that is dependent on the differences of molecular weights and specific heats ratios between fluids. It is also found that the pressure oscillation ratio is significantly decreasing with a very small value (varying to 0 from 0.5) or a very large value (varying to 1 from 0.5) of vu, and is $o(\Delta M \Delta\gamma)$ but not $o(\Delta\gamma)^2$ as reported by Karni and Abgrall [3]. To more clearly show that, Eq. (69) can be rewritten in terms of specific heats (at constant volume) instead of molecular weights as below

$$\frac{p_1^1 - p}{p_1^1} = -\frac{vu(1-vu)(C_{vL}(\gamma_L - 1) - C_{vR}(\gamma_R - 1))(\gamma_R - \gamma_L)}{(vuC_{vL}(\gamma_L - 1) + (1-vu)C_{vR}(\gamma_R - 1))(vu(\gamma_R - 1) + (1-vu)(\gamma_L - 1))}. \tag{70}$$

From the above equation, one can see that the pressure oscillation rate is not $o(\Delta\gamma)^2$ but it is that only if $C_{vR} = C_{vL}$.

As for the conventional *gamma model*, the same approach as above is applied. We have an additional equation for the direct computation of specific heats ratio for the mixture as

$$(\rho\gamma)_j^{n+1} = (\rho\gamma)_j^n + \delta(\rho\gamma), \tag{71}$$

where

$$\delta(\rho\gamma) = -v\Delta(\rho\gamma u). \tag{72}$$

Considering the same flow problem as above, with the initial data

$$W_j^0 = \begin{cases} \left(\rho, \rho u, \frac{1}{\gamma_L - 1}p + \frac{\rho}{2}u^2, \rho\gamma_L\right), & j < 1, \\ \left(\rho, \rho u, \frac{1}{\gamma_R - 1}p + \frac{\rho}{2}u^2, \rho\gamma_R\right), & j \geqslant 1. \end{cases} \tag{73}$$

Following the same lines for the TCFC model and thermodynamic model as above, we have

$$\begin{aligned} \rho_1^1 &= \rho, \\ u_1^1 &= u, \\ \gamma_1^1 &= vu\gamma_L + (1-vu)\gamma_R, \\ E_1^1 &= \left(\frac{vu}{\gamma_L - 1} + \frac{1-vu}{\gamma_R - 1}\right)p + \frac{1}{2}\rho u^2. \end{aligned} \tag{74}$$

Substituting the expression of E_1^1 in Eq. (74) into the equation of state (55) (in terms of γ), we obtain the same formulation as that in Eq. (66). From the expression of γ_1^1 in Eq. (74), we have

$$\frac{1}{\gamma_1^1 - 1} = \frac{1}{vu\gamma_L + (1-vu)\gamma_R - 1} = \frac{vu}{\gamma_L - 1} + \frac{1-vu}{\gamma_R - 1} - \frac{vu(1-vu)(\gamma_R - \gamma_L)^2}{(\gamma_R - 1)(\gamma_L - 1)(vu\gamma_L + (1-vu)\gamma_R - 1)}. \tag{75}$$

From Eqs. (66) and (75), one can obtain

$$\begin{aligned} &\left(\frac{vu}{\gamma_L - 1} + \frac{1-vu}{\gamma_R - 1}\right)p_1^1 - \left(\frac{vu(1-vu)(\gamma_R - \gamma_L)^2}{(\gamma_R - 1)(\gamma_L - 1)(vu\gamma_L + (1-vu)\gamma_R - 1)}\right)p_1^1 \\ &\quad = \left(\frac{vu}{\gamma_L - 1} + \frac{1-vu}{\gamma_R - 1}\right)p. \end{aligned} \tag{76}$$

Eq. (76) can be rewritten as

$$\frac{p_1^1 - p}{p_1^1} = \frac{vu(1-vu)(\gamma_R - \gamma_L)^2}{(vu\gamma_L + (1-vu)\gamma_R - 1)(vu(\gamma_R - 1) + (1-vu)(\gamma_L - 1))}. \tag{77}$$

If $0 < vu < 1$, from the above equation it can be seen that the newly computed pressure $p_1^1 \neq p$, therefore a pressure oscillation is also generated in this case. The oscillation rate has the value as that of the term at the right hand of Eq. (77) and has a definite sign (positive). Similarly, it is also found that the pressure oscillation ratio is significantly decreasing with a very small value (varying to 0 from 0.5) or a very large value (varying to 1 from 0.5) of vu, and is $o(\Delta\gamma)^2$ as reported by Karni and Abgrall [3] but for the mass fraction model (thermodynamic model).

We have done the analysis of the proposed TCFC model and conventional conservative models on the simple structure of isolated contact interfaces, it is shown that our model produces a uniform pressure field across the material fronts and the pressure maintains in equilibrium near the contact interfaces. The results also show that both two conventional conservative models do not maintain the pressure equilibrium across contact interfaces and the pressure oscillation rate for gamma model is $o(\Delta\gamma)^2$ and for thermodynamic model is $o(\Delta M \Delta\gamma)$ which is different from that of $o(\Delta\gamma)^2$ reported by Karni and Abgrall. They are the same only if the specific heats of fluids (at constant volume) are equal. The pressure oscillation rates for both models have a definite sign with a monotonous sign for the gamma model but maybe not for the thermodynamic (or mass fraction) model. From the analysis, it can be seen that the conclusions are consistent with that obtained from a general viewpoint of numerical uncertainty analysis in the last section.

We have now three models that will be used for the simulation of several test problems in this paper. One is the conventional "gamma" model with Eqs. (1)–(3) and (8). The set of governing Eqs. (1)–(3), (5), combined with (6) or (7) is the conventional "thermodynamic" model. The set of governing Eqs. (1), (2) and (16), combined with Eqs. (26) and (34) (or only Eq. (44)) is the proposed TCFC model with the direct calculation of the γ-value of the mixture for the best description of multicomponent or multifluid flows.

4. Numerical solution of the governing equations

As mentioned in the introduction, we use a Godunov method based upon a fast exact Riemann solver to solve the system of governing equations in this paper, though any kind of numerical schemes applicable for the solution of hyperbolic equations could be used.

4.1. Godunov method

Godunov [23,24] proposed a first-order accurate scheme for the solution of the governing Eqs. (1)–(3), which can be written in conservative form in one dimension as

$$\mathbf{U}_i^{n+1} = \mathbf{U}_i^n + \frac{\Delta t}{\Delta x}\left[\mathbf{F}_{i-(1/2)} - \mathbf{F}_{i+(1/2)}\right] \tag{78}$$

with intercell numerical flux given by

$$\mathbf{F}_{i+(1/2)} = \mathbf{F}\left(\mathbf{U}_{i+(1/2)}(0)\right) \tag{79}$$

where $\mathbf{U}_{i+(1/2)}(0)$ is the local Riemann solution at the cell interface position $i + (1/2)$ of the conservation laws (1)–(3) in one dimension with initial conditions given by

$$\mathbf{U}(x,0) = \mathbf{U}^0(x) = \begin{cases} \mathbf{U}_i^R & \text{if} \quad x < 0, \\ \mathbf{U}_{i+1}^L & \text{if} \quad x > 0, \end{cases} \tag{80}$$

where

$$\mathbf{U}_i^{\mathrm{R}} = \mathbf{U}_i^n, \quad \mathbf{U}_{i+1}^{\mathrm{L}} = \mathbf{U}_{i+1}^n. \tag{81}$$

This has first-order accuracy. To improve the accuracy of the scheme, the first-order Godunov method can be extended to second, and even higher order by using the basic concepts of Van Leer [59] (see Toro [58] for an overall description of different higher order schemes). This approach has become known as the MUSCL technique. Here our main concern is the demonstration of the proposed model, so, for brevity, the second-order scheme is adequate. We use the piecewise linear MUSCL approach for the data reconstruction to achieve second-order accuracy. Then we have

$$\mathbf{U}_i^{\mathrm{L}} = \mathbf{U}_i^n - \frac{1}{2}\Delta_i, \quad \mathbf{U}_i^{\mathrm{R}} = \mathbf{U}_i^n + \frac{1}{2}\Delta_i, \tag{82}$$

where $\mathbf{\Delta}_i$ is the flux slope defined as

$$\mathbf{\Delta}_i = \frac{1}{2}(1+\omega)\Delta\mathbf{U}_{i-\frac{1}{2}} + \frac{1}{2}(1-\omega)\Delta\mathbf{U}_{i+\frac{1}{2}}, \tag{83}$$

and, as usual,

$$\Delta\mathbf{U}_{i-\frac{1}{2}} \equiv \mathbf{U}_i^n - \mathbf{U}_{i-1}^n, \qquad \Delta\mathbf{U}_{i+\frac{1}{2}} \equiv \mathbf{U}_{i+1}^n - \mathbf{U}_i^n. \tag{84}$$

ω is a free parameter in the real interval $[-1, 1]$. For $\omega = 0$, $\mathbf{\Delta}_i$ is a central-difference approximation, multiplied by Δx, to the first spatial derivative of the numerical solution at time step n (that is what we use in this paper). To suppress possible spurious oscillations, we use the so-called ''minbee'' slope limiter. The details can be found in [58].

4.2. Pike's exact Riemann solver

For a complete solution, the fluxes in the above Godunov scheme, at each intercell position, should be determined using a Riemann solver. Although many kinds of exact or approximate Riemann solvers have been developed, e.g. [9,14,19,21,24,25,38,42,45,47,51,55,57] since the pioneering work of Godunov [23], Pike's Riemann solver [42] seems to us to be the fastest to date. In Pike's Riemann solver, the equations for the Riemann problem for a perfect gas are rewritten in terms of three similarity parameters and a weak dependence on the ratio of specific heats of the gases. First we define some dimensionless variables as

$$P_{\mathrm{L}} = \frac{p^*}{p_{\mathrm{L}}}, \quad P_{\mathrm{R}} = \frac{p^*}{p_{\mathrm{R}}}, \tag{85}$$

$$U_{\mathrm{L}} = \frac{u_{\mathrm{L}} - u^*}{c_{\mathrm{L}}}, \quad U_{\mathrm{R}} = \frac{u^* - u_{\mathrm{R}}}{c_{\mathrm{R}}}, \tag{86}$$

where $P_{\mathrm{L}}, P_{\mathrm{R}}$ and $U_{\mathrm{L}}, U_{\mathrm{R}}$ are the dimensionless pressures and velocities on the left and right sides of the initial discontinuity, respectively. p, u are the real pressure and velocity and the subscripts L, R and the superscript * stand for the left side, right side and star region, respectively. Here c denotes a modified sound speed defined as

$$c = \frac{a}{\gamma}, \quad a = \sqrt{\frac{\gamma p}{\rho}}, \tag{87}$$

where a is the real sound speed and γ is the ratio of specific heats. The subscripts L, R are ignored in some of the following equations for brevity. The relationships between the velocity, density, and pressure for the constant regions between the waves can be rewritten in terms of the above dimensionless flow variables as

$$U(P,\gamma)=\begin{cases}\frac{(P-1)(1+g)^{1/2}}{(P+g)^{1/2}}, & P\geqslant 1,\\ \frac{\left(P^{G}-1\right)}{G}, & P<1,\end{cases} \tag{88}$$

where g and G are functions of γ given by

$$g=\frac{\gamma-1}{\gamma+1},\quad G=\frac{\gamma-1}{2\gamma}. \tag{89}$$

Further, if we define the density ratios as

$$R_{\mathrm{L}}=\frac{\rho_{\mathrm{L}}^{*}}{\rho_{\mathrm{L}}},\quad R_{\mathrm{R}}=\frac{\rho_{\mathrm{R}}^{*}}{\rho_{\mathrm{R}}}, \tag{90}$$

we have the density ratio in terms of the pressure ratio given by

$$R=\begin{cases}(P+g)/(1+Pg), & P\geqslant 1,\\ P^{1-2G}, & 0\leqslant P\leqslant 1.\end{cases} \tag{91}$$

Three main similarity parameters are introduced as

$$p_r=\frac{p_{\mathrm{R}}}{p_{\mathrm{L}}}, \tag{92}$$

$$\lambda=\frac{c_{\mathrm{R}}}{c_{\mathrm{L}}+c_{\mathrm{R}}}, \tag{93}$$

$$\mathrm{d}u=\frac{u_{\mathrm{L}}-u_{\mathrm{R}}}{c_{\mathrm{L}}+c_{\mathrm{R}}}, \tag{94}$$

and two subsidiary parameters γ_{L} and γ_{R} are also used. In terms of these parameters, the Riemann solution requires P and U to satisfy

$$P_{\mathrm{L}}=p_rP_{\mathrm{R}}, \tag{95}$$

$$\mathrm{d}u=(1-\lambda)U_{\mathrm{L}}+\lambda U_{\mathrm{R}}, \tag{96}$$

where $U(P,\gamma)$ is given by Eq. (88), or alternatively $P(U,\gamma)$ is given by the inverse form

$$P=\begin{cases}1+U\left\{U/2(1+g)+\sqrt{\left[1+U^2/4(1+g)^2\right]}\right\}, & U\geqslant 0,\\ (1+GU)^{1/G}, & -1/G\leqslant U\leqslant 0,\\ 0, & U\leqslant -1/G.\end{cases} \tag{97}$$

There are two simple approximate Riemann solvers developed for the estimation of the guessing values for the exact iterative Riemann solver in [42]. They are the two-expansion approximation (TE) and the two-shock approximation (TS) given by

$$P_{\mathrm{L}}=\frac{p_r+\left[1-\lambda(1-p_r)\right]^2}{1+p_r}(1+\mathrm{d}u/4)^4 \tag{98}$$

for two-expansion waves and

$$P_{\mathrm{L}} = c + 2d\left(d + \sqrt{c + d^2 + g_p}\right), \tag{99}$$

where

$$c = \frac{(1-\lambda)(1+g_{\mathrm{L}})^{1/2} + \lambda(1+g_{\mathrm{R}})^{1/2} p_r^{1/2}}{(1-\lambda)(1+g_{\mathrm{L}})^{1/2} + \lambda(1+g_{\mathrm{R}})^{1/2}/p_r^{1/2}}, \tag{100}$$

$$d = \frac{\mathrm{d}u}{2(1-\lambda)(1+g_{\mathrm{L}})^{1/2} + 2\lambda(1+g_{\mathrm{R}})^{1/2}/p_r^{1/2}}, \tag{101}$$

$$g_p = \begin{cases} g_{\mathrm{R}} p_r, & p_r \leqslant 1, \\ g_{\mathrm{L}}, & p_r > 1, \end{cases} \tag{102}$$

for two shock waves. The combination of the above two approximations (called TETS) approximations can be used for the estimation of guess values for the exact solution of the Riemann problem. A fast, exact Riemann solver was developed [42] in which a second-order "look-up" method was implemented. An error function for the iterative process is defined from (96) to be

$$E = \mathrm{d}u - (1-\lambda)U_{\mathrm{L}} - \lambda U_{\mathrm{R}}. \tag{103}$$

Expanding E in a Taylor series in terms of p^* and after some rearrangements and simplifications, we obtain a fast iterative procedure as below

$$P_{\mathrm{L}}^{(n+1)} = P_{\mathrm{L}}^{(n)}\left(1 - \frac{E}{2P_{\mathrm{L}}E'}\right)^2, \tag{104}$$

where

$$\frac{E}{P_{\mathrm{L}}E'} = \frac{\mathrm{d}u - (1-\lambda)U_{\mathrm{L}} - \lambda U_{\mathrm{R}}}{-(1-\lambda)(PU')_{\mathrm{L}} - \lambda(PU')_{\mathrm{R}}} \tag{105}$$

and

$$PU' = \begin{cases} \frac{P}{2}\left(\frac{1+g}{P+g}\right)^{1/2}\left(1 + \frac{1+g}{P+g}\right), & P \geqslant 1, \\ P^G = 1 + GU, & P < 1, \end{cases} \tag{106}$$

where U is calculated by Eq. (88) with a guess value or the previous value of P.

This concludes our brief review of first- and second-order accurate Godunov schemes and a fast, exact Riemann solver. The combination of the Godunov scheme described above and Pike's fast exact Riemann solver provides an efficient solver for the solution of the hyperbolic system of conservation laws presented in the previous section. The present solver is successfully applied to the simulation of multicomponent flows with the proposed TCFC model and other conventional models. Several test examples will be presented in the next section.

5. Numerical experiments

Here we present some numerical results from four test cases to illustrate our proposed TCFC model and the fast exact Riemann solver-based Godunov method, to compare the proposed model with existing conventional conservation models, and to show that it can handle both strong and weak shocks. Also, we want to check if the numerical solutions obtained with the proposed TCFC model and conventional conservation models converge to the correct weak ones. For brevity, we use G model, T model, and H model in all of the following plots to refer to the conventional gamma model, the conventional thermodynamic model, the proposed TCFC model, respectively. In all of the following four test cases, the CFL [17] number is taken to be 0.6.

Test A: We consider a shock tube initially filled with two different gases having different specific heat ratios. A similar problem has been considered by Larrouturou [32], Abgrall [2], Karni [30], Cocchi and Saurel [12]. But the data for the test problem we consider here is taken from [2] (in SI units) since it shows a strong shock. Consider a shock tube with a length of 1.0 m, including two chambers, separated by a fictitious diaphragm at 0.5 m from either end of the tube. Two initial constant states are defined as

Test A:

$$\begin{array}{llllll} x < 0.5, & \rho_{\mathrm{L}} = 14.54903, & u_{\mathrm{L}} = 0.0, & p_{\mathrm{L}} = 194.3 \times 10^5, & \gamma_{\mathrm{L}} = 1.67, & C_{v\mathrm{L}} = 2420, \\ x \geqslant 0.5, & \rho_{\mathrm{R}} = 1.16355, & u_{\mathrm{L}} = 0.0, & p_{\mathrm{R}} = 1.0 \times 10^5, & \gamma_{\mathrm{R}} = 1.4, & C_{v\mathrm{R}} = 732. \end{array}$$

The results shown are obtained using the first- and second-order exact-Riemann-solver-based Godunov scheme with the three different models. The mesh has 200 cells. Fig. 1(a)–(e) shows the density, pressure, velocity, internal energy and the ratio of specific heats at time $t = 200$ μs using the first-order method. Fig. 1(f) shows an enlargement of the variation of the ratio of specific heats in the region across the contact discontinuity. From the figures, one can see that there is a large spread in the density and internal energy profiles due to the numerical diffusion of the method. A dip in the density and a smaller one in the internal energy across the contact interface are clearly visible with the thermodynamic model. It can also be seen that there is a large difference in the γ-profile between the thermodynamic model, gamma model and the proposed TCFC model. It seems that the overshoot of the γ-value for the thermodynamic model results in a large undershoot of the density and internal energy. To improve the accuracy of the first-order method and avoid the effect of large numerical diffusion, a second-order method can be used. Fig. 2(a)–(e) shows the results for the different models: significant improvement on the accuracy is achieved. Very smooth distributions of pressure and velocity are obtained with all three models. In [2], a visible, small undershoot of the velocity with the conventional conservation model, and a visible, small overshoot in the velocity with the quasi-conservative model were obtained using Roe's scheme. A large dip in the density, in Fig. 2(a), and a very small dip in the internal energy, in Fig. 2(d), are visible with the conventional thermodynamic model. A very small dip in the density with the conventional gamma model is obtained that is almost invisible in Fig. 2(a). But with the proposed TCFC model, completely oscillation-free results are obtained for the density, pressure, velocity and internal energy. The reason why these models behave differently can be sought from the γ-profile. From Fig. 2(f) one can see that the γ-value obtained with the conventional thermodynamic model is much larger than that obtained with the conventional gamma model and the proposed TCFC model. For this test case, the γ-value obtained with the gamma model is very close to that for the proposed model: so, even though the model is flawed (as shown in Sections 2 and 3) it still works, for this particular problem, with a fully conservative numerical scheme. From this test problem, one can see that the conventional thermodynamic model shows a large undershoot in the density, due to the inconsistent and inaccurate calculation of the γ-value. The conventional gamma model behaves much better, except for an almost invisible dip in the density, despite its

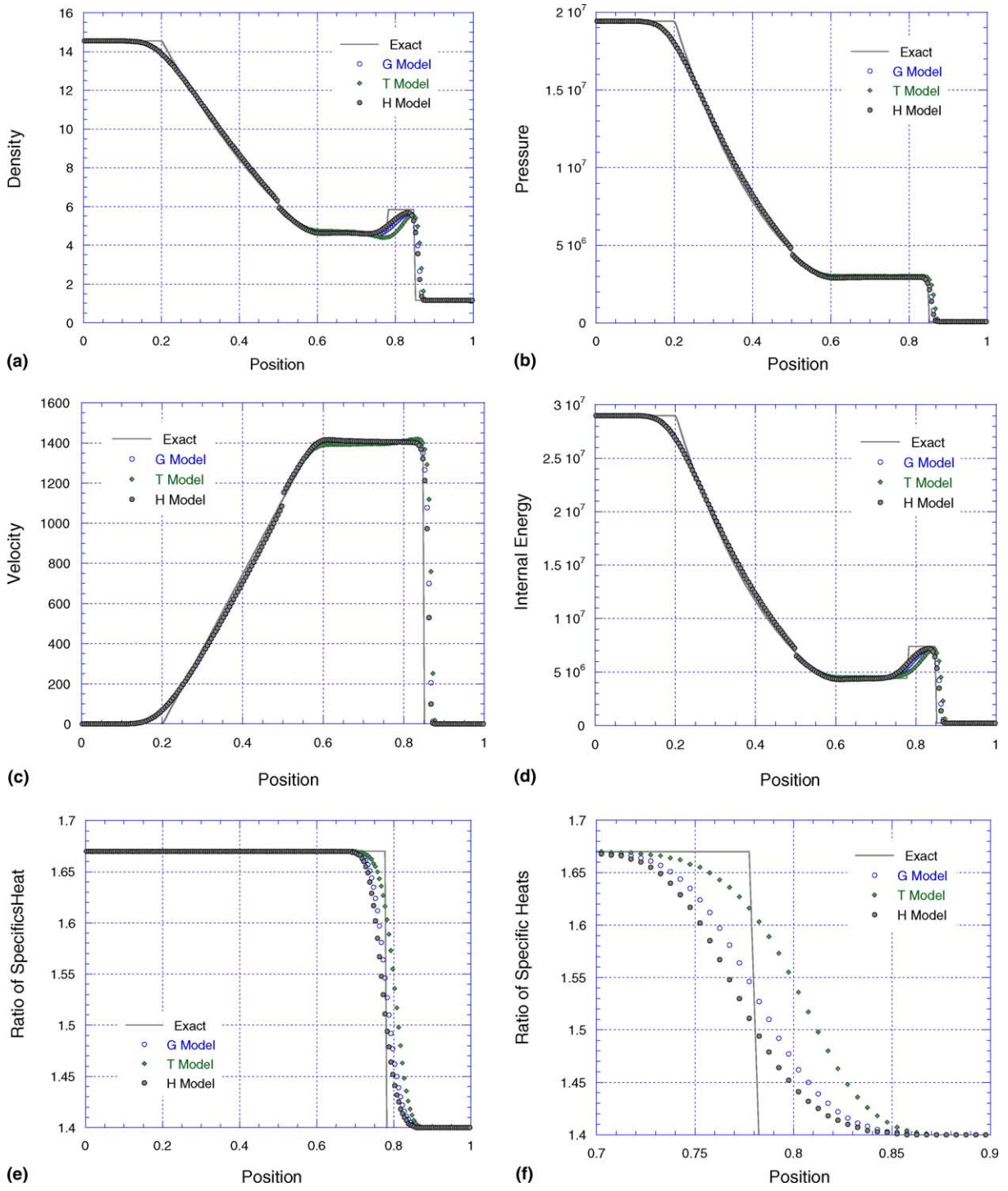

Fig. 1. Results for a shock tube with two different gases using the three models and a first-order scheme at time $t = 200$ μs with 200 mesh cells: solid line is the exact solution; ○, "gamma" model; ◆, "thermodynamic" model; ●, "TCFC" model. (a) Density, (b) pressure, (c) velocity, (d) internal energy, (e) ratio of specific heats, (f) zoom of specific heats ratio.

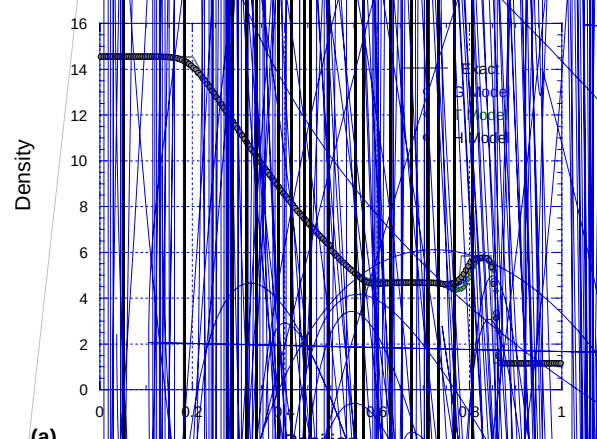

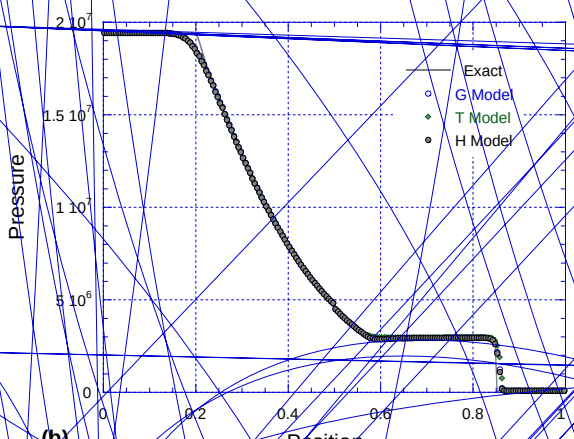

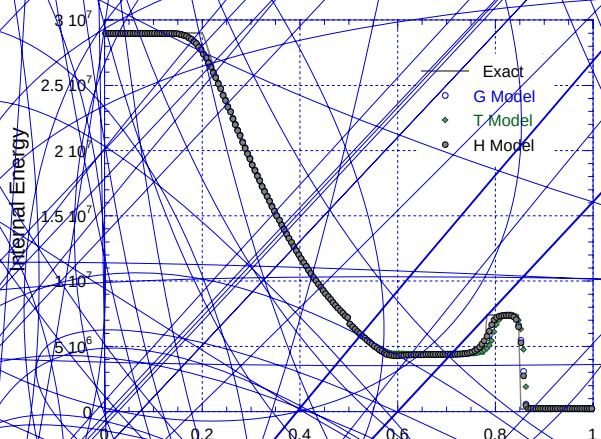

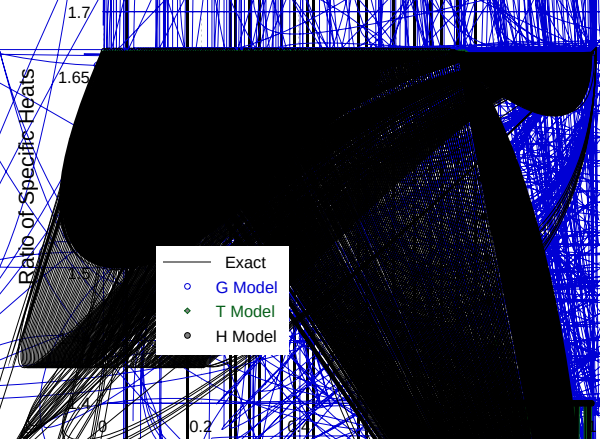

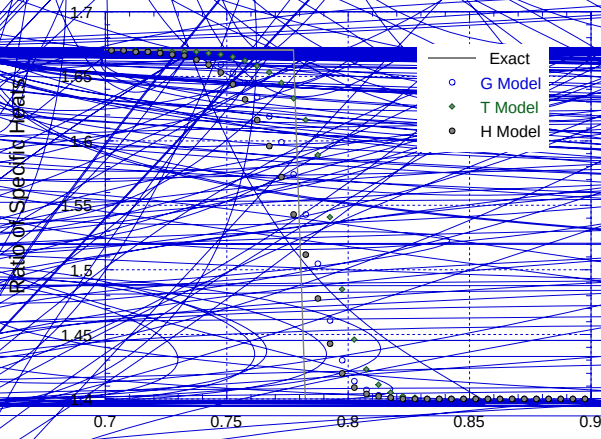

Fig. 2. Results for a shock tube with two dif… three models and a second-order scheme at time $t = 200$ μs with 200 mesh cells: solid line is the exact solution; ○, ◆, "thermodynamic" model; ●, "TCFC" model. (a) Density, (b) pressure, (c) velocity, (d) internal energy, (e) ratio of specific heats, (f) zoom of specific heats ratio.

intrinsic flaw. The proposed TCFC model gives essentially oscillation-free results for all variables. It should be pointed out that, using the present solver, an undershoot appeared only in the density, with the conventional models while an undershoot was also obtained in the velocity, for the same problem, with Roe's scheme [2]. That means that some numerical schemes could have an amplifying effect of the error if the model is flawed.

Test B: The second test problem we present is Karni and Quirk's test case (cited in [2]). Abgrall [2] showed a simulation based on a quasi-conservative approach and a conventional conservation model. It consists of a shock tube filled with air, where a shock wave moves to the right. In the pre-shock state, a slab of helium is located between $x = 0.4$ m and $x = 0.6$ m. The shock wave is initially located at $x = 0.25$ m. The initial conditions and properties are given as

Test B:

$$0.0 \leqslant x \leqslant 0.25, \quad \rho = 1.3765, \quad u = 0.3948, \quad p = 1.57, \quad \gamma = 1.40 \quad C_v = 0.72,$$

$$\begin{matrix} 0.25 \leqslant x < 0.4, \\ 0.6 \leqslant x \leqslant 1.0, \end{matrix} \quad \rho = 1.0000, \quad u = 0.0000, \quad p = 1.00, \quad \gamma = 1.40, \quad C_v = 0.72,$$

$$0.4 \leqslant x < 0.60, \quad \rho = 0.1380, \quad u = 0.0000, \quad p = 1.00, \quad \gamma = 1.67, \quad C_v = 2.42,$$

where the density, velocity and pressure are measured in CGS units as indicated in [2]. The results are obtained using a second-order Godunov method with the three different models. The grid has 400 cells. Fig. 3(a)–(e) shows the density, pressure, velocity, internal energy and the ratio of specific heats, respectively, at time $t = 0.3$ s. From these plots, one can see that the three different models have almost the same behavior, except for the conventional "thermodynamic" model that gives a small overshoot in the pressure and internal energy in the slab region. No spurious oscillations can be seen in the plots of all variables for all three models, with the present fast, exact Riemann solver-based Godunov method. Fig. 3(f) shows a detail of the change in γ near the interfaces for the different models. One can see that the ratio of specific heats has very close values for all the models, except for the thermodynamic model: for this model, a small overshoot in the value of γ results in a small overshoot in the pressure and the internal energy. But, unlike for Test A, in this case most of the spread due to numerical diffusion only occurs on one side of the contact interface. No spurious oscillations of flow variables were obtained across the contact interfaces. Abgrall [2] showed spurious oscillations of the pressure distribution using Roe's scheme with a conventional conservation model (we are not sure which one was used but we guess that it was either the thermodynamic or the gamma model). The comparison of the present results with those in [2] gives us confidence that the spurious oscillations of the pressure distribution obtained in [2] are related to the selected numerical scheme but not to the selected model.

Test C: The third test problem is one we formulated to produce a weak post-shock contact discontinuity by hitting a material interface with a strong shock wave. Consider a shock tube that consists of a stationary interface at $x = 0.5$ m separating argon and nitrogen, and a right-traveling shock wave ($M_s = 3.352$) initially located at $x = 0.25$ m. The initial conditions and properties are defined as

Test C:

$$\begin{matrix} 0 \leqslant x < 0.25, & \rho = 5.1097, & u = 738.6, & p = 1398737, & \gamma = 1.67, & C_v = 208.1, \\ 0.25 \leqslant x < 0.5, & \rho = 1.62286, & u = 0.000, & p = 101325, & \gamma = 1.67, & C_v = 208.1, \\ 0.5 \leqslant x \leqslant 1.0, & \rho = 1.13802, & u = 0.000, & p = 101325, & \gamma = 1.401, & C_v = 296.8, \end{matrix}$$

where the density, velocity and pressure are measured in SI units. We use 400 cells to solve this problem. The distributions of density, pressure, velocity, and internal energy are obtained using the

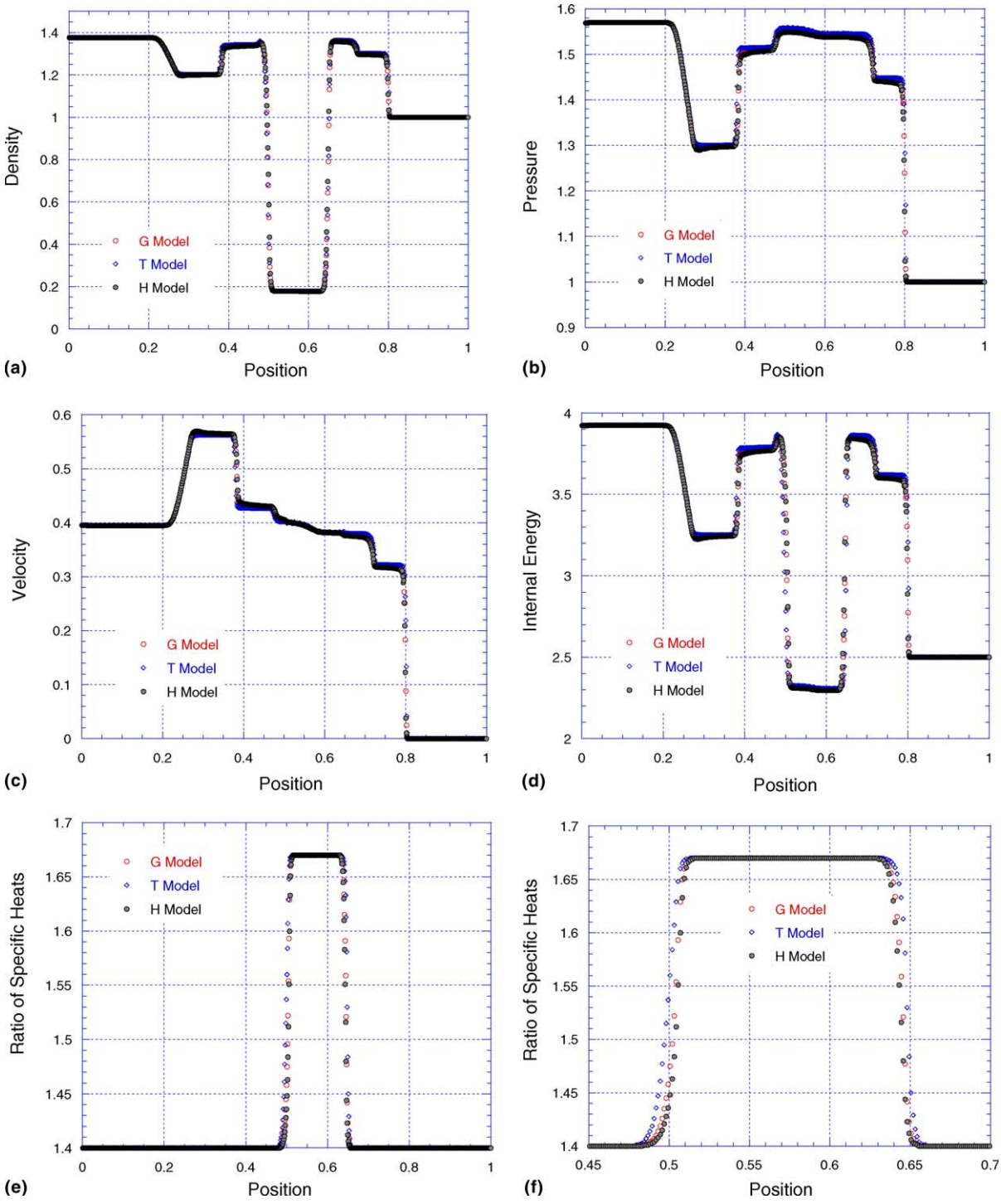

Fig. 3. Results for a right-travelling shock wave hitting a helium slab in an air-filled shock tube using the three models and a second-order scheme at time $t = 0.3$ μs with 400 mesh cells: ○, "gamma" model; ◆, "thermodynamic" model; ●, "TCFC" model. (a) Density, (b) pressure, (c) velocity, (d) internal energy, (e) ratio of specific heats, (f) zoom of specific heats ratio.

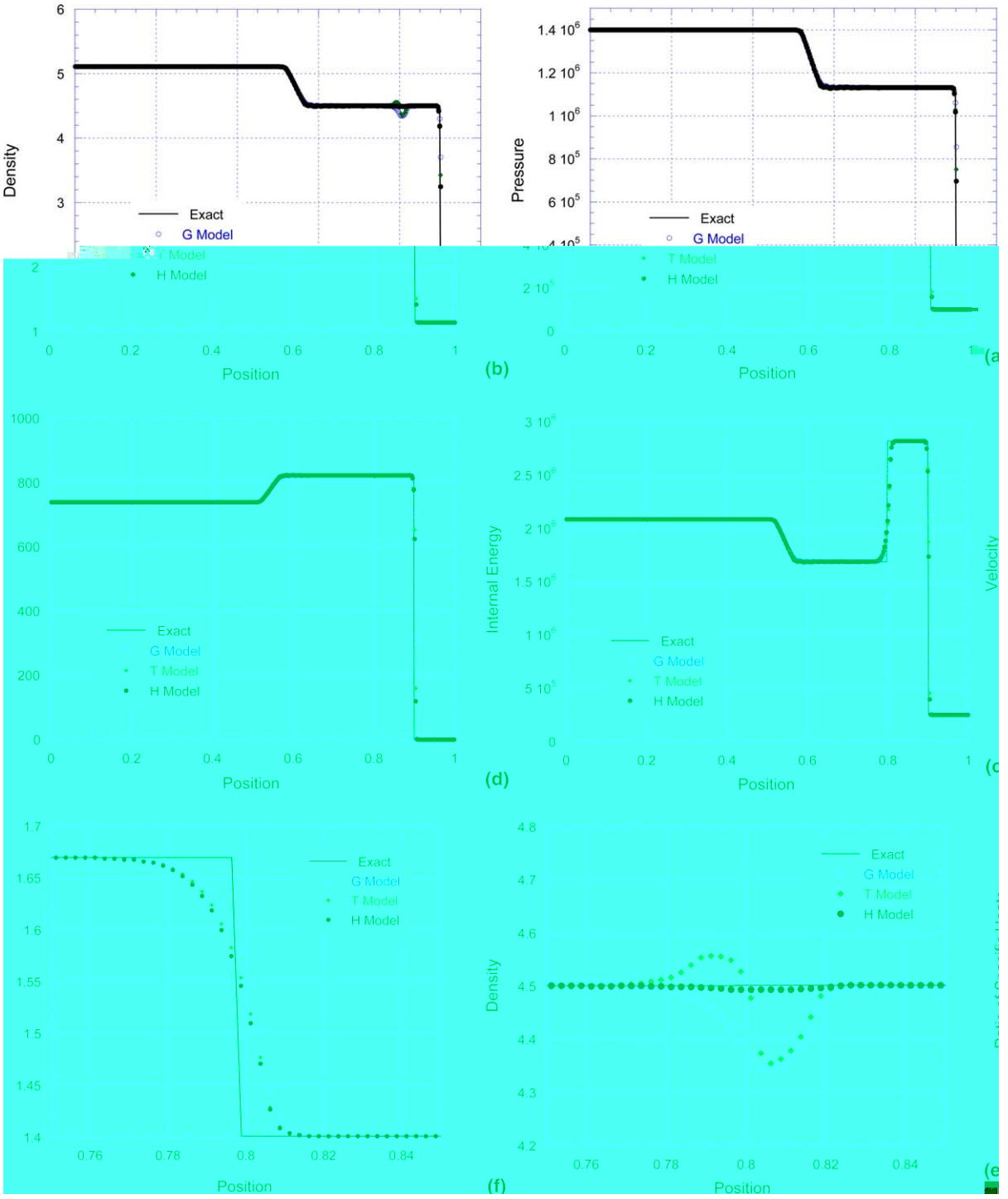

Fig. 4. Results for a strong right-travelling shock wave hitting an argon-nitrogen interface in a shock tube using the three models and a second-order scheme at time $t = 600$ μs with 400 mesh cells: solid line is the exact solution; ○, "gamma" model; ◆, "thermodynamic" model; ●, "TCFC" model. (a) Density, (b) pressure, (c) velocity, (d) internal energy, (e) zoom of specific heats ratio, (f) zoom of density distribution.

second-order-accurate Godunov method with the three different conservation models. Fig. 4(a)–(d) shows the results at time $t = 600$ μs. From these plots, one can see that very smooth results are obtained for pressure, velocity and internal energy for all three conservation models. A completely oscillation-free distribution of density across the interface is obtained with the proposed TCFC model, but a large bump and a large dip in the density, on the left and right side of the interface, respectively, can be seen for the other two models. Fig. 4(f) shows a detail of the density distribution near the interface computed with the different models. It can be clearly seen that the conventional gamma model gives a large dip in the density in the interface region. The conventional thermodynamic model produces a large bump on the left side of the interface and a large dip on the right side. However, the proposed TCFC model gives a very smooth snapshot of the density distribution. Spurious oscillations are completely eliminated with the TCFC model and the comparison between the obtained numerical results and the corresponding exact solutions looks excellent, at such small scale. Fig. 4(e) gives a detail of the γ-distribution near the interface: one can see that the conventional gamma model produces a larger γ that results in a large undershoot in the density. The γ-value obtained by the conventional thermodynamic model is very close with slightly higher value, compared with the proposed TCFC model. Even though the difference in the γ values with different models is not very large, it still produces a large difference in the density profiles. The plot in Fig. 4(e) looks similar to those in Fig. 2(e)–(f) from Test A: a spread in the γ-distribution due to numerical diffusion occurs across the interface. The conventional conservation models fail for this kind of problems with strong shocks. But Test C is more instructive than Test A because the conventional gamma model also produced a large error in density profile.

Test D. Finally, we consider a shock-contact surface interaction problem that has been studied by Abgrall [2], Karni [30] and Shyue [52] for verifying convergence of the numerical solutions to the correct weak ones. The problem we consider here consists of a stationary interface, initially at $x = 0.5$ separating two different gases. The initial two constant states are defined as [2]

Test D:

$$\begin{aligned} &0.0 \leqslant x < 0.5, \quad \rho = 1.0, \quad u = 0.00, \quad p = 10.0, \quad \gamma = 1.6, \\ &0.5 \leqslant x \leqslant 1.0, \quad \rho = 2.0, \quad u = -1.0, \quad p = 0.10, \quad \gamma = 1.4. \end{aligned}$$

Since this problem is just studied numerically, we assume that the two specific heats C_{v1}, C_{v2} have the same value and no units are specified for the variables (not given in [2]). The problem is solved using the present second-order-accurate Godunov method, with the three conservation models and 200 mesh points. Fig. 5(a)–(e) shows the distributions of density, pressure, velocity, internal energy and the ratio of specific heats at time $t = 0.3$: no spurious oscillations can be seen in any of the profiles, for all of three conservation models. Furthermore, Fig. 5(f), a detail of the γ-profiles near the interface, shows that the γ-values obtained by the three different models are very close, with a slightly higher value for the conventional conservation models. The spread of the γ-profiles due to numerical diffusion occurs on only one side of the interface, similarly to the results of Test B. Again, for this kind of problem, one can obtain good results even with the conventional conservation models. Fig. 6(a) shows a density profile obtained by the proposed TCFC model with different mesh points and a corresponding detail is shown in Fig. 6(b). From these plots, we can see that the computed solutions with the present TCFC model have excellent convergence to the correct weak ones. The same conclusion could actually be reached for the other three conservation models; for brevity, the results are not shown here for the convergence test. We show the results of Test D with all three conservation models to stress that this test case is not sufficient to be used for model validation. Although the conventional conservation models are incorrect, they still give excellent results, having good agreement with the analytical solutions since the value of γ does not change within an expansion fan or across a shock.

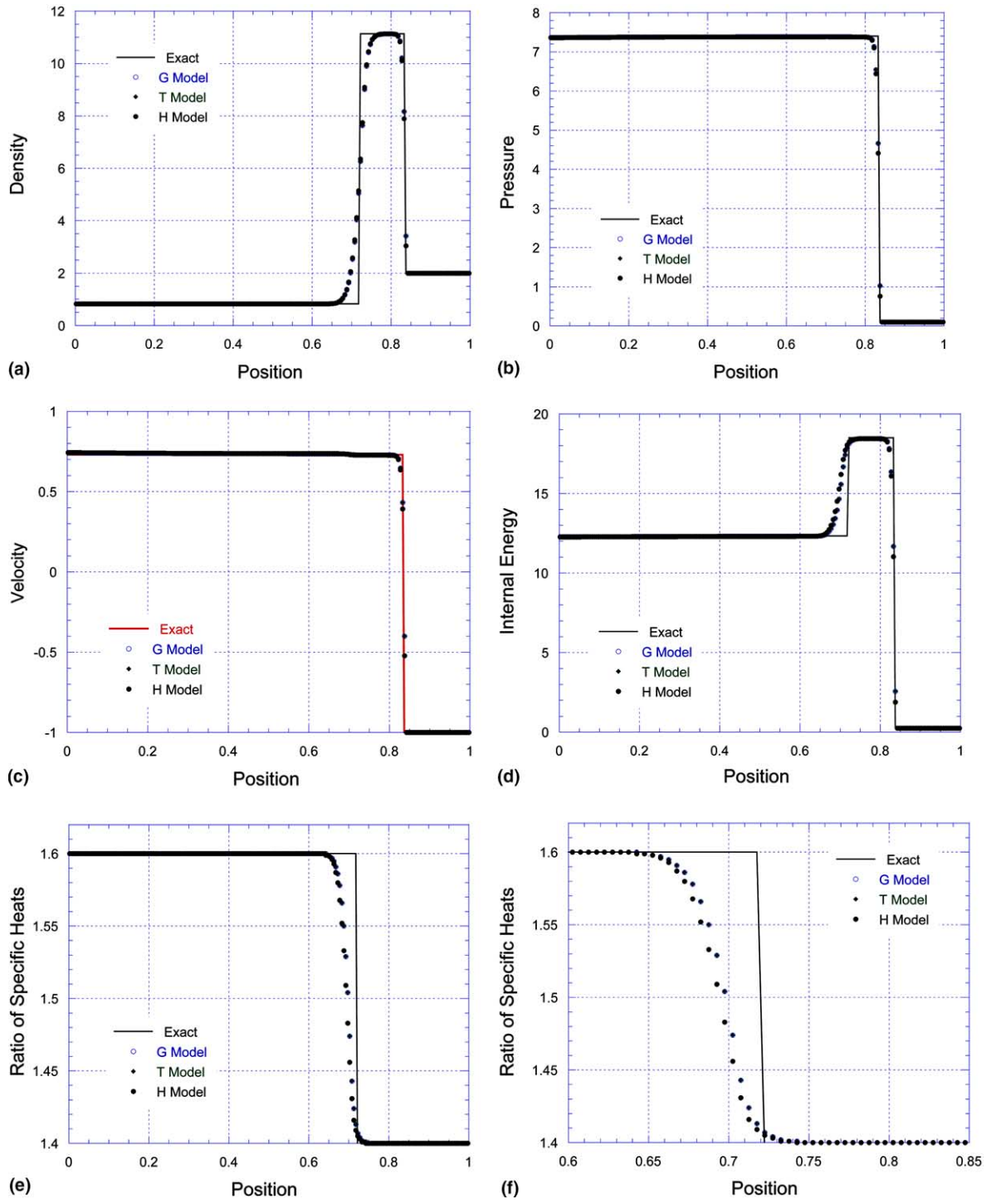

Fig. 5. Results for a shock-contact surface interaction in a shock tube using the three models and a second-order scheme at time $t = 0.3$ μs with 200 mesh cells: solid line is the exact solution; ○, "gamma" model; ◆, "thermodynamic" model; ●, "TCFC" model. (a) Density, (b) pressure, (c) velocity, (d) internal energy, (e) ratio of specific heats, (f) zoom of specific heats ratio.

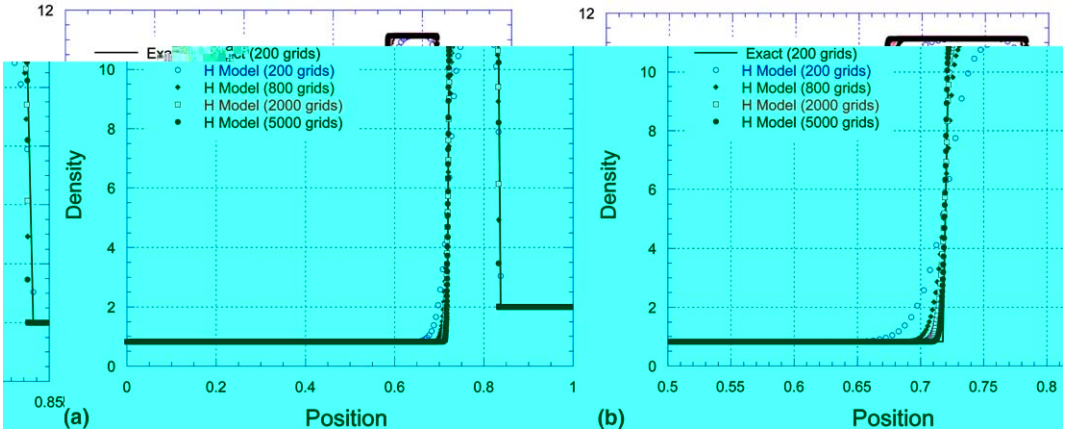

Fig. 6. Results for the convergence study of a shock-contact surface interaction in a shock tube using the TCFC model and a second-order scheme at time $t = 0.3$ μs with different mesh cells: solid line is the exact solution with 200 mesh cells; ○, 200 mesh cells; ◆, 800 mesh cells; □, 2000 mesh cellzs; ●, 5000 mesh cells. (a) Density distribution, (b) zoom of density distribution.

6. Conclusions

We have presented a new, fully conservative treatment of contact discontinuities based upon the theory of numerical uncertainties and the concept of the total energy conservation of the mixture for compressible, multicomponent flows. The proposed TCFC models provide the best description of multicomponent or multifluid flows, and have been successfully implemented with a fast, exact Riemann solver-based Godunov method. The models have been successfully tested with the numerical experiments presented in this paper: they show that the proposed TCFC models are able to handle both strong and weak shocks. Essentially oscillation-free results are obtained for all variables in all test cases. The proposed TCFC models belong to the conservative approaches and independent of numerical schemes, they are compatible with existing non-conservative and quasi-conservative approaches in the simulation of compressible multicomponent flows associated with shock waves and contact discontinuities.

The analysis of the numerical uncertainties indicates that conventional conservation models, like the gamma and thermodynamic models, use an incorrect procedure for the calculation of the mixture's ratio of specific heats. This is why they produce unphysical results in the simulation of compressible multicomponent flows with strong shocks, especially in the cases with both weak post-shock contact discontinuities and strong shock waves. The conservative or non-conservative form of the governing equations is not the ultimate reason that produces oscillating solutions near material interfaces.

The analysis of the proposed TCFC model and conventional conservative models on the pressure evolution for a mixture associated with isolated contact interfaces gives consistent conclusions with that obtained from a general viewpoint of numerical uncertainty analysis. It is shown that the proposed TCFC model produces a uniform pressure field across the material fronts and the pressure maintains in equilibrium near the contact interfaces. The results also show that both two conventional conservative models do not maintain the pressure equilibrium across contact interfaces and the pressure oscillation rate for gamma model is $o(\Delta\gamma)^2$ and for thermodynamic model is $o(\Delta M \Delta\gamma)$ which is different from that of $o(\Delta\gamma)^2$ reported by Karni and Abgrall. They are the same only if the specific heats of fluids (at constant volume) are equal. The pressure oscillation rates for both models have a definite sign with a monotonous sign for the gamma model but maybe not for the thermodynamic (or mass fraction) model.

But numerical experiments also indicated that the conventional gamma model is still applicable to problems with weak shocks and problems with both strong shocks and strong post-shock contact

discontinuities. The conventional thermodynamic model is also applicable to the problems with weak shocks. The last two conclusions seem to conflict with the results obtained using Roe's scheme with one of the conventional models [2]. These latter suggest that the unphysical results obtained with an incorrect model might also be related to the selected numerical scheme.

From the present numerical results, one can also see that the problems with weak shocks and strong post-shock contact discontinuities are not suitable for the validation of the models for multicomponent flows. The capability of handling strong shocks and weak post-shock contact discontinuities seems more critical to the demonstration of any model for compressible multicomponent or multifluid flows.

It is noteworthy to note that in most cases the oscillations observed are in the profiles of density and velocity as well as energy (some time) but not pressure which seems a conflict with the theoretical analysis in the literature, so whether the pressure equilibrium is a main argument or not, or how does the pressure evolution play a role in the simulation of this problem needs to be further investigated.

The extensions to the simulation of multidimensional problems and flows of compressible dissimilar liquids and gas-liquid mixture have been undertaken. Some results have been announced in [64,65] and the details will be reported in forthcoming papers.

Acknowledgements

The authors thank the anonymous reviewers for their valuable and constructive comments on the paper, particularly for their suggestion on the addition of an analysis of TCFC models on the pressure evolution for a mixture associated with isolated contact interfaces. This work was supported in part by the United States Department of Energy under Contract No. DE-FG02-97ER54413.

References

[1] R. Abgrall, Generalization of Roe scheme for the computation of mixture of perfect gases, Rech. Aerosp. 6 (1988) 31–43.
[2] R. Abgrall, How to prevent pressure oscillations in mutlicomponent flow calculations: a quasi conservative approach, J. Comput. Phys. 125 (1996) 150–160.
[3] R. Abgrall, S. Karni, Computations of compressible multifluids, J. Comput. Phys. 169 (2001) 594–623.
[4] G. Allaire, S. Clerc, S. Kokh, A five-equation model for the simulation of interfaces between compressible fluids, J. Comput. Phys. 181 (2002) 577–616.
[5] M.H. Anderson, B.P. Puranik, J.G. Oakley, P.W. Brooks, R. Bonazza, Shock tube investigation of hydrodynamic issues related to inertial confinement fusion, Shock Waves 10 (2000) 377–387.
[6] Y.C. Chang, T.Y. Hou, B. Merriman, S. Osher, A level set formulation of Eulerian interface capturing methods for incompressible fluid flows, J. Comput. Phys. 124 (1996) 449–464.
[7] D. Chargy, R. Abgrall, L. Fezoui, B. Larrouturou, Comparisons of several upwind schemes for multicomponent one dimensional inviscid flows, INRIA Rep. 1253 (1990).
[8] I.L. Chern, J. Glimm, O. McBryan, B. Plohr, S. Yaniv, Front tracking for gas dynamics, J. Comput. Phys. 62 (1986) 83–110.
[9] A.J. Chorin, Random choice solutions of hyperbolic systems, J. Comput. Phys. 22 (1976) 517–533.
[10] J.F. Clark, S. Karni, J.J. Quirk, P.L. Roe, L.G. Simmonds, E.F. Toro, Numerical computation of two-dimensional unsteady detonation waves in high-energy solids, J. Comput. Phys. 106 (1993) 215–233.
[11] J.P. Cocchi, R. Saurel, J.C. Loraud, Treatment of interface problems with Godunov-type scheme, Shock Waves 5 (1996) 347–357.
[12] J.P. Cocchi, R. Saurel, A Riemann problem based method for the resolution of compressible multimaterial flows, J. Comput. Phys. 137 (1997) 265–298.
[13] P. Collela, P.R. Woodward, The piecewise parabolic method (PPM) for gas-dynamical simulations, J. Comput. Phys. 54 (1984) 174–201.
[14] P. Collela, H.M. Glaz, Efficient solution algorithm for the Riemann problem for the real gases, J. Comput. Phys. 59 (1985) 264–289.
[15] P. Collela, R.E. Ferguson, H.M. Glaz, Multifluid algorithms for Eulerian finite difference methods (preprint), 1994.
[16] C.H. Cooke, T.J. Chen, Continuous front tracking with subsell resolution, J. Sci. Comput. 6 (1991) 269–282.

[17] R. Courant, K.O. Friedrichs, Supersonic Flow and Shock Waves, Wiley–Interscience, New York, 1948.
[18] S.F. Davis, An interface tracking method for hyperbolic systems of conservation laws, Appl. Numer. Math. 10 (1992) 447–472.
[19] P. Dutt, A Riemann solver based on a global existence proof for the Riemann problem, Technical Report ICASE 86-3, NASA Langley Research Center, USA, 1986.
[20] R.P. Fedkiw, T. Aslam, B. Merriman, S. Osher, A non-oscillatory Eulerian approach to interfaces in multimaterial flows (the ghost fluid method), J. Comput. Phys. 152 (1999) 457–492.
[21] P. Glaister, An efficient algorithm for compressible flows with real gases, Int. J. Numer. Methods Fluids 9 (1269) (1989) 1269–1283.
[22] J. Glimm, J. Grove, X.L. Li, K.-M. Shyue, Y. Zeng, Q. Zhang, Three dimensional front tracking, SIAM J. Sci. Comput. 19 (1998) 703–727.
[23] S.K. Godunov, A finite-difference method for the computation of discontinuous solutions of the equations of fluid dynamics, Mat. Sb. 47 (1959) 271–295.
[24] S.K. Godunov (Ed.), Numerical Solution of Multidimensional Problems in Gas Dynamics, Nauka Press, Moscow, 1976.
[25] J.J. Gottlieb, C.P.T. Groth, Assessment of Riemann solvers for unsteady one-dimensional inviscid flows of perfect gases, J. Comput. Phys. 78 (1988) 437–458.
[26] J. Grove, R. Menikoff, The anomalous reflection of a shock wave at a material interface, J. Fluid Mech. 219 (1990) 313–336.
[27] A. Harten, ENO schemes with subcell resolution, J. Comput. Phys. 83 (1989) 148–184.
[28] T.Y. Hou, Le Floch, Why nonconservative schemes converge to wrong solutions – error analysis, Math. Comput. 62 (206) (1994) 497–530.
[29] P. Jenny, B. Mueller, H. Thomann, Correction of conservative Euler solvers for gas mixtures, J. Comput. Phys. 132 (1997) 91–107.
[30] S. Karni, Multicomponent flow calculations by a consistent primitive algorithm, J. Comput. Phys. 112 (1994) 31–43.
[31] S. Karni, Hybrid multifluid algorithms, SIAM J. Sci. Comput. 17 (1996) 1019–1039.
[32] B. Larrouturou, How to preserve the mass fractions positivity when computing compressible multicomponent flows, J. Comput. Phys. 95 (1991) 59–84.
[33] B. Larrouturou, L. Fezoui, On the equations of multicomponent perfect or real gas inviscid flow, in nonlinear hyperbolic problems, in: C. Carasso, P. Charrier, B. Hanouzet, J.-L. Joly (Eds.), Lecture Notes in Mathematics, vol. 1402, Springer, New York/Berlin, 1989.
[34] R.J. LeVeque, K.-M. Shyue, One dimensional front tracking based on high resolution wave propagation methods, SIAM J. Sci. Comput. 16 (1995) 348–377.
[35] X.-D. Liu, R.P. Fedkiw, M.J. Kang, A boundary condition capturing method for Poisson's equation on irregular domains, J. Comput. Phys. 160 (2000) 151–178.
[36] D.-K. Mao, A treatment of discontinuities for finite difference methods in the two-dimensional case, J. Comput. Phys. 104 (1993) 377–397.
[37] D.-K. Mao, A treatment of discontinuities for finite difference methods, J. Comput. Phys. 103 (1992) 359–369.
[38] R. Menikoff, B. Plohr, The Riemann problem for fluid flow of real materials, Rev. Mod. Phys. 61 (1989) 75–130.
[39] G.H. Miller, E.G. Puckett, A higher-order Godunov method for multiple condensed phases, J. Comput. Phys. 128 (1996) 134–164.
[40] W. Mulder, S. Osher, J.A. Sethian, Computing interface motion in compressible gas dynamics, J. Comput. Phys. 100 (1992) 209–228.
[41] S. Osher, Convergence of generalized MUSCL schemes, SIAM J. Numer. Anal. 22 (1985) 947–961.
[42] J. Pike, Riemann solvers for perfect and near-perfect gases, AIAA J. 31 (1993) 1801–1808.
[43] Y.X. Ren, S.P. Wang, Q.S. Liu, M.Y. Shen, A higher-order and non-oscillating finite volume method for hyperbolic conservation laws using spline interpolation, in: Proceedings of the 5th National Fluid Dynamics Conference, Beijing, May 1995.
[44] Y.X. Ren, Q.S. Liu, S.P. Wang, M.Y. Shen, A high order accurate, non-oscillating finite volume scheme using spline interpolation for solving hyperbolic conservation laws, Acta Aerodynamica Sinica 14 (1996) 281–287.
[45] P.L. Roe, Approximate Riemann solvers, parameter vectors and difference schemes, J. Comput. Phys. 43 (1981) 357–372.
[46] P.L. Roe, Technical Report, Cranfield Institute of Technology, 1984 (unpublished).
[47] R. Saurel, M. Larini, J.C. Loraud, Exact and approximate Riemann solvers for real gases, J. Comput. Phys. 112 (1994) 126–137.
[48] R. Saurel, R. Abgrall, A simple method for compressible multifluid flows, SIAM J. Sci. Comput. 21 (1999) 1115–1145.
[49] R. Saurel, R. Abgrall, A multiphase Godunov method for compressible multifluid and multiphase flows, J. Comput. Phys. 150 (1999) 425–467.
[50] R. Saurel, O. Lemetayer, A multiphase model for compressible flows with interfaces, shocks, detonation waves and cavitation, J. Fluid Mech. 431 (2001) 239–271.
[51] V. Schleicher, Ein einfaches und effizientes verfahren zur loesung des Riemann-problems, Z. Flugwiss. Weltraumforsch. 17 (1993) 265–269.
[52] K.-M. Shyue, An efficient shock-capturing algorithm for compressible multicomponent problems, J. Comput. Phys. 142 (1998) 208–242.
[53] K.-M. Shyue, A fluid-mixture type algorithm for compressible multicomponent flow with van der Waals equation of state, J. Comput. Phys. 156 (1999) 43–88.

[54] K.-M. Shyue, A fluid-mixture type algorithm for compressible multicomponent flow with Mie–Gruneisen equation of state, J. Comput. Phys. 171 (2001) 678–707.
[55] J. Smoller, Shock Waves and Reaction Diffusion Equations, Springer, Berlin, 1994.
[56] V. Ton, Improved shock-capturing methods for multicomponent and reacting flows, J. Comput. Phys. 128 (1996) 237–253.
[57] E.F. Toro, A fast Riemann solver with constant covolume applied to the Random choice method, Int. J. Numer. Methods Fluids 9 (1989) 1145–1164.
[58] E.F. Toro, Riemann Solvers and Upwind Methods for Fluid Dynamics, Springer, New York/Berlin, 1997.
[59] B. van Leer, Towards the ultimate conservative difference scheme V. A second-order sequel to Godunov's method, J. Comput. Phys. 32 (1979) 101–136.
[60] S.P. Wang, L. Jiang, M.Y. Shen, Hyperbolic spline method: theory and applications, in: Proceedings of the Beijing Workshop on Computational Fluid Dynamics, vol. 5, Beijing, 1993, pp. 41–51.
[61] S.P. Wang, Y.X. Ren, L. Jiang, Y.B. Zeng, On the uncertainty problems in the simulations of fluid flow and heat transfer, in: Proceedings of the CSET Fluid Machinery Conference, vol. V, Huangshan, China, 1994, pp. 1–7.
[62] S.P. Wang, L. Jiang, M.Y. Shen, Tension spline numerical method for solving high R_a number natural convection problem, Acta Aerodynamica Sinica 14 (1996) 7–12.
[63] S.P. Wang, Treatments of contact discontinuities in compressible multi-material flows, March 2001 (unpublished).
[64] S.P. Wang, M.H. Anderson, J.G. Oakley, and R. Bonazza, An efficient and high-resolution solver for the two-dimensional numerical simulation of the Richtmyer–Meshkov instability, presented at the 8th International Workshop on the Physics of Compressible Turbulent Mixing (8th IWPCTM), California Institute of Technology, Pasadena, California, USA, Dec. 9–14, 2001.
[65] S.P. Wang, J. Oakley, M. Anderson, R. Bonazza, 2002, Modeling of 2-phase, multi-species flows with shock-interface interactions, presented at the 2002 ANS Winter Meeting, Washington, DC, November 17–21, 2002.
[66] K. Xu, BGK-based scheme for multicomponent flow calculations, J. Comput. Phys. 134 (1997) 122–133.